1-1-2001

The silicon (100) surface and its organic modifications

Yousung Jung
Iowa State University

The silicon (100) surface and its organic modifications

by

Yousung Jung

A thesis submitted to the graduate faculty

in partial fulfillment of the requirements for the degree of

MASTER OF SCIENCE

Major: Physical Chemistry

Program of Study Committee:
Mark S. Gordon, Major Professor
James W. Evans
Gordon J. Miller

Iowa State University

Ames, Iowa

2001

Graduate College
Iowa State University

This is to certify that the Master's thesis of

Yousung Jung

has met the thesis requirements of Iowa State University

Signatures have been redacted for privacy

TABLE OF CONTENTS

CHAPTER 1. GENERAL INTRODUCTION

Surfaces usually have some characteristics different than the bulk portion, and this unique feature of surfaces is the key to understanding and utilizing them properly. The silicon surface is one of the most extensively studied subjects over the past decades because of its industrial importance as semiconductor materials.[1-3] Modification of the silicon surface is also becoming very popular to develop new functional surfaces and molecular devices.[4] Organic molecules are typically being used to achieve this goal. By introducing the organic functional groups to the surface, surfaces can obtain additional properties such as biological functionality, optical activity, etc.[5] However, the complexity of interfacial surfaces makes this modification very difficult. Thus, in order to accomplish this goal, a detailed understanding of the surface at a molecular level is critical.

One of the most widely used and powerful experimental techniques in surface chemistry is STM (scanning tunneling microscopy). STM can give atomically resolved real time images. However, the molecular level picture of surfaces including the structural information is difficult to obtain from the STM experiments only. In addition, even though the other experimental tools such as IR, ultraviolet photoelectron spectroscopy (UPS), high resolution electron energy loss spectroscopy (HREELS), etc. can give additional useful information for many surface reactions, it is still hard to thoroughly describe the surface reactions by experiments only. Accordingly, theoretical calculations are essential and usually performed along with the experiments to elucidate the surface phenomena more clearly.

The Si(100) surface is one of the most well studied and technologically important silicon surfaces. Many experimental and theoretical studies showed that the silicon surface is dimerized when the crystal is cut along the (100) direction. This is called reconstruction of the silicon surface. The reconstructed Si(100) has a pair of dangling bonds (two unpaired electrons) at each surface dimer, and these two dangling bonds of each dimer leave the surface very reactive. Through this entire process of reconstruction (dimerization), the surface becomes have (2×1) periodicity, denoted by Si(100)-(2×1).

Another interesting aspect of Si(100), from the theoretical point of view, is that the dimers have significant diradical character in a singlet state. In order words, the single determinant methods such as restricted Hartree-Fock (RHF) and density functional theory (DFT) are not relevant to correctly describe the Si(100) surface because of this partial diradical character. Since the first demonstration of this feature of Si(100) by Redondo and Goddard,[6] it has been confirmed by many authors afterwards.[7,8] On the other hand, there are also some open issues, for example, the structure of Si(100). The dimers of the reconstructed Si(100) surface can either be symmetric or bucked. Many experimental evidences and some theoretical calculations, especially using the DFT method, support the buckling of the dimers,[9-13] while other theoretical calculations predict the opposite, the symmetric structure as a minimum.[6-8, 14-17] Investigating and hopefully providing some insight regarding this question is one of the purposes of this thesis.

Theoretical calculations for surfaces are usually performed using either slab or cluster models. The slab approach models the actual surface using periodic boundary conditions with a repeating unit cell (a slab). The advantage of this approach is that the edge effect can be eliminated, while the disadvantage is that the Hamiltonain in slab calculations is limited to DFT which may not always be the proper choice. On the other hand, the main advantage of using the cluster approach is that the high level quantum mechanical methods can be used systematically as long as the size of the cluster is affordable. However, the edge effect due to a finite size of the cluster is still a problem in the cluster approach.

A hybrid QM/MM (quantum mechanics/molecular mechanic) method has been developed to reduce the edge effect in the cluster model, while still being able to use the high level quantum chemical methods such as perturbation theory and coupled cluster. The main idea of the QM/MM approach is that only chemically active region is treated by quantum mechanics and a chemically inactive region (for example, the bulk or the solvent) by inexpensive molecular mechanics. By performing the forcefield calculations for the chemically inactive part, really a big system can be applied to the QM/MM method reducing the edge effect. The SIMOMM (surface integrated molecular orbital molecular mechanics)[18] is the surface QM/MM method modified based on the IMOMM (integrated molecular orbital molecular mechanics)[19] scheme. Details about the SIMOMM method will be described in

chapter 5, and this SIMOMM method will be effectively used throughout this thesis for large cluster calculations.

Thesis organization

The main topic of this thesis is the Si(100) surface and some surface reactions on it. The thesis is organized as follows: The structure of the Si(100) surface is first discussed in chapter 2. Then, the adsorption reactions of water and benzene on Si(100) are presented in chapter 3 and 4, respectively. The Hessian module of the SIMOMM method was modified, and the results appear in chapter 5. Each chapter (chapter 2-4) subsequent to this general introduction is actually a paper, which will be or has already been published. At the end of the thesis, a general conclusion will be drawn briefly.

References

1. H. N. Waltenburg and J. T. Yates, Jr., Chem. Rev. **95**, 1589 (1995)
2. M. J. Sailor and E. J. Lee, Adv. Mater. **9**, 783 (1997)
3. C. H. Choi and M. S. Gordon, *The Chemistry of Functional Groups* series edited by Saul Patai and Zvi Rappoport (in press)
4. J. M. Buriak, J. Chem. Soc. Chem. Commun., 1051 (1999)
5. G. P. Lopinski, D. J. Moffatt, D. D. M. Wayner, R. A. Wolkow, Am. Chem. Soc. **122**, 3548 (2000)
6. A. Redondo, and W. A. Goddard III, J. Vac. Sci. Technol. **21**, 344 (1982)
7. B. Paulus, Surf. Sci. **375**, 55 (1997)
8. J. Shoemaker, J. W. Burggraf, and M. S. Gordon, J. Chem. Phys. **112**, 2994 (2000)
9. R. A. Wolkow, Phy. Rev. Lett. **68**, 2636 (1992)
10. E. Landemark, C. J. Karlsson, Y. –C. Chao, and R. I. G. Uhrberg, Phys. Rev. Lett. **69**, 1588 (1992)
11. P. C. Weakliem, G. W. Smith, and E. A. Carter, Surf. Sci. **232**, L219 (1990)
12. N. Roberts and R. J. Needs, Surf. Sci. **236**, 112 (1990)
13. J. S. Hess, and D. J. Doren, J. Chem. Phys. **113**, 9353 (2000)
14. R. M. Tromp, R. J. Hamers and J. E. Demuth, Phys. Rev. Lett. **55**, 1303 (1985)
15. Z. Jing and J. L. Whitten, Surf. Sci. **274**, 106 (1992)
16. T. Hoshino, M. Hata, S. Oikawa, M. Tsuda, Phys. Rev. B **54**, 11331 (1996)
17. M. S. Gordon, J. R. Shoemaker, and L. W. Burggraf, J. Chem. Phys. **113**, 9355 (2000)
18. J. Shoemaker, L. W. Burggarf, and M. S. Gordon, J. Phys. Chem. A **103**, 3245 (1999)
19. F. Maseras and K. Morokuma, J. Comput. Chem. **16**, 1170 (1995)

CHAPTER 2. AN *AB INITIO* STUDY OF THE STRUCTURE OF THE Si(100) SURFACE USING TWO- AND THREE-DIMER CLUSTERS

A paper to be submitted to Main Group Chemistry

Yousung Jung, Kenneth D. Jordan[‡], and Mark S. Gordon

Abstract

Two- and three-dimer cluster models were used to elucidate the structures of small models of the Si(100) surface. Because surface dimers have been shown to have significant singlet diradical character, multi-reference wave functions were used in order to obtain a reliable description of such species.[9,12] CASSCF (complete active space SCF) geometry optimizations find symmetric structures to be the global minima, with no local minima at buckled structures. This result for the three-dimer cluster implies that dimer-dimer interactions play no significant role in determining the structure of these species. These results are in contrast with most previous calculations that predict buckling of surface dimers. The effect of the dynamic part of electron correlation on surface structure was assessed by performing single point multi-reference perturbation theory (MRMP) calculations along the three buckling normal modes. The MRMP results are in qualitative agreement with the CASSCF predictions. The implications of these results with regard to the structure of the Si(100) surface are discussed.

Introduction

The Si(100) surface has been the subject of many experimental and theoretical studies[1-7] due to its importance in the semiconductor industry. These studies have revealed many aspects of the silicon surface including the fact that the Si(100) surface reconstructs, after being cleaved, to form dimers. The experimental bond length of the dimer (2.26 Å) suggests that the Si-Si bonding in this species is between a single and double bond.[29] Several computational studies have demonstrated that these dimers have significant diradical character with ~1/3 of an electron occupying the lowest unoccupied molecular orbital

[‡] Department of Chemistry, University of Pittsburgh, Pittsburgh, Pennsylvania 15260.

(LUMO) in each dimer. This suggests that single-determinant wave functions (e.g., Hartree-Fock, density functional theory) are unlikely to provide a reliable description of the structure and bonding of such species. It is therefore essential, when using clusters to describe the Si(100) surface, to use a proper wave function as a starting point. This is particularly true when one considers such questions as:

(i) Are the Si(100) surface dimers buckled or symmetric?

(ii) Does dynamic correlation play an important qualitative role in determining the structure of the surface?

(iii) Do dimer-dimer interactions affect the structure of the surface?

Electron correlation energy is defined as the difference between the "exact" energy and the energy at the Hartree-Fock limit, achieved by using an infinite basis set. Non-dynamic (or internal) correlation refers to the electron correlation that can be recovered by adding flexibility to the wave function, when there are near degeneracies (i.e., low-lying excited states) or when the gap between HOMO and LUMO is small enough to permit configurational mixing. The MCSCF (multi-configurational SCF)[8] method is typically used for recovering the non-dynamic electron correlation. The remaining error relative to the exact energy is called dynamic correlation, even though there is no rigorous way to separate these two effects. Perturbation theory and configuration interaction (CI) are the most common methods to account for dynamic correlation.

Redondo and Goddard[9] were the first to show that, because surface dimers exhibit partial diradical character (significant population of the LUMO), a single reference wave function is not sufficient for an adequate description of the Si(100) dimerized surface, and a multi-reference (e.g., MCSCF) wave function is necessary. A simple way to determine whether or not a system needs a multi-reference wave function is to examine the restricted Hartree-Fock (RHF) orbital energies. When the LUMO orbital energy is negative, the system is frequently multi-configurational and needs a non-dynamic electron correlation correction. Indeed, this is the case for the reconstructed Si(100) surface. Recent studies[9-12] using MCSCF-based methods have predicted that that the Si(100) surface dimers are symmetric (or 'unbuckled'), while single reference methods such as Hartree-Fock or density functional

theory (DFT)[13-16,26] have generally predicted the only potential energy minimum to be a buckled structure.

Recently, Hess and Doren[13] argued that dynamic correlation plays a significant role in determining the structure of the surface and even alters the relative stabilities of buckled and symmetric structures to favor a buckled structure. They optimized a Si_9H_{12} single dimer cluster with both DFT and complete active space (CAS) SCF including 4 electrons in four orbitals, CASSCF(4,4), methods. They found that DFT optimization gives a buckled structure, while CASSCF(4,4) optimization predicts a symmetric (C_{2v}) structure as a minimum. Single point MRMP calculations at both the DFT-optimized buckled structure and the CASSCF-optimized symmetric structure predicted the buckled structure to be slightly lower (0.9 kcal/mol) in energy than the symmetric one. Based on these single point MRMP calculations, they concluded that the structure of Si_9H_{12} is buckled and dynamic correlation plays an important role in determining the structure. Of course, a comparison of energies of two different geometries that were obtained from different levels of theory may not be reliable, especially where the energy difference is quite small.

Ideally, one should optimize the structure of the clusters at the MRMP level of theory in order to include the effects of both dynamic and non-dynamic correlation on the predicted structure. Unfortunately, MRMP analytic gradients are not yet available. One alternative is to distort the cluster along the CASSCF buckling mode(s) and perform MRMP calculations along the resulting potential energy curve. Following the procedure for the single dimer Si_9H_{12} cluster, Gordon, Shoemaker, and Burggraf found that the MRMP energy increases monotonically along the buckling mode, qualitatively in agreement with CASSCF results. They also performed a single reference MP2 geometry optimization starting from both symmetric and buckled structures, and found only a symmetric dimer structure. They therefore concluded that the Si(100) surface is symmetric within a Si_9H_{12} cluster model at 0 K, and that dynamic correlation does not have a qualitatively important effect on the predicted geometry.

It has also been some suggested[14-16] that interactions between the two dimers in the same row may have a stabilizing effect on the bucked structure. These DFT calculations indicate that a buckled structure gains extra stability due to dimer-dimer interactions (one Si

atom of a dimer is pointing up and the other pointing down in one dimer, with adjacent dimers buckled in the opposite direction). This stabilization has been estimated to be 1.5~3 kcal/mol per dimer in a two-dimer model and 3.5~4.5 kcal/mol in a three-dimer cluster model. On the contrary, recent multi-reference CI calculations using a two-dimer cluster model[10] still predict a symmetric structure as a minimum, implying that dimer-dimer interactions play little role in determining the structure of the surface. Thus, there is some disagreement between DFT and MCSCF results regarding whether the dimer-dimer interaction affects the dimer structure.

One may also question whether a cluster of any size can adequately model the Si(100) surface and if so, what an appropriate cluster size might be? An alternative approach, the slab model using periodic boundary conditions, is considered to be size-independent and thus more representative of the surface site interactions than the cluster model, as long as the supercell of the slab model maintains a reasonable periodicity. A recent DFT study on H_2 desorption from the Si(100) surface using both slab and cluster models[23] showed that a three-dimer cluster already converges to the results predicted by to the slab model.

Since, to the best of our knowledge, a three-dimer cluster has not yet been studied using the combined the MCSCF and MRMP methods, the present work examines the structure of the surface systematically by increasing the size of the cluster (the number of dimers) up to three dimers, in order to provide some insight regarding the effect of dimer-dimer interactions, if any, on the structure of the surface dimers. As an extension of the Si_9H_{12} cluster study[11,12], two-dimer ($Si_{15}H_{16}$) and three-dimer ($Si_{20}H_{21}$) clusters are analyzed with CASSCF(4,4) and CASSCF(6,6) wave functions, respectively.

Computational details

Two-dimer ($Si_{15}H_{16}$) and three-dimer ($Si_{20}H_{21}$) clusters were used to model the structure of the Si(100) surface. The 6-31G(d)[28] basis set was used for the $Si_{15}H_{16}$ cluster, and the HW(d) effective core potential (ECP) basis set was used for $Si_{20}H_{21}$ due to the size of the cluster. It has been shown in many papers[11,17,18] that HW(d)[19] is a reasonable basis set for the study of the silicon surface, since it saves considerable computational cost by treating the

core electrons of heavy atoms with fitted potentials and still gives reasonable results. HW(d) means the 3-21G(d) basis for the valence shell electrons of Si atoms and the –21G basis for H atoms.

Four active electrons and four active orbitals were used as an active space in the MCSCF[8] calculations for the two-dimer cluster, denoted by CASSCF(4,4), and six electrons and six orbitals, CASSCF(6,6), for the three-dimer cluster. All of these active orbitals correspond to bonding and anti-bonding Si-Si surface dangling bond orbitals. The optimized structures were characterized by computing and diagonalizing the Hessian matrices (matrix of energy second derivatives with respect to the nuclear coordinates). A minimum has a positive definite hessian and a transition state (or first order saddle point) has one negative eigenvalue. As discussed below, single point calculations were performed with second order multi-reference perturbation theory (MRMP2).[32]

The GAMESS electronic structure program[20] was used for all calculations reported here, making use of the parallel MCSCF codes.[21,22]

Results and discussion

Both two-dimer and three-dimer clusters are predicted to have only symmetric C_{2v} minima on their respective CASSCF potential energy surfaces. Starting from buckled structures predicted by density functional theory, CASSCF optimizes to symmetric dimers. These one-[12], two-, and three-dimer results, particularly the three-dimer cluster, further suggest that dimer-dimer interactions play little role in determining the surface structure.

The dimer bond lengths as a function of the size of the cluster are compared in Table 1. All cluster models using MCSCF wave functions predict the dimer bond length to be between 2.24~2.28 Å very close to the experimental value (~2.26 Å). In fact, since the Si_9H_{12} results suggest that ECP's underestimate the dimer distance by 0.04 Å, it is likely that CASSCF/6-31G(d) consistently predicts a distance of 2.28 Å. In constrast, the RHF method[11] predicts a much smaller value of 2.18 Å. Because RHF (and other single determinant methods) cannot occupy the antibonding LUMO, the Si-Si bonding in the dimer is overestimated by over-emphasizing the Si-Si π bonding. On the other hand, a singlet UHF

calculation yields a dimer Si-Si bond length of 2.32 Å, closer to the experimental value than RHF. The fact that the singlet UHF is distinct from the RHF wave function for this species, and the large spin contamination both suggest that a single configuration description is inadequate. Thus, we conclude that the bond length of the Si(100) surface dimer is independent of the size of the cluster model as long as an adequate multi-reference wave function is used.

The effect of dynamic electron correlation on the structure of the surface was investigated by calculating single point MRMP energies along the buckling vibrational normal modes. The symmetric structures found in the CASSCF geometry optimization were used for the vibrational frequency calculations. The number of buckling modes is equal to the number of surface dimers included in the calculation. Table 2 summarizes the CASSCF and MRMP2 results along each buckling mode. The main point that can be drawn from this table is that both CASSCF and MRMP2 energies monotonically increase as the surface dimers buckle along the buckling normal modes. In other words, MRMP2 does not change the qualitative CASSCF trend that the surface dimers are symmetric and increase in energy as the dimers buckle. The only quantitative difference is that the relative MRMP2 energies are somewhat (not greatly) lower than the relative CASSCF energies. Therefore, at this point, we conclude that dynamic correlation does not play a major role in determining the structure of the surface dimers.

A more detailed analysis of the dimer-dimer interactions was obtained by examining the localized CASSCF active orbitals (LMOs) for the three-dimer cluster, using the Ruedenberg energy localization procedure.[33,34] As noted by Ruedenberg and co-workers,[33,34] localization of CASSCF orbitals leads to atomic-like orbitals. It is then possible to examine both the density matrix elements connecting these hybrid LMOs and the Coulomb and exchange repulsions between them. The former interactions provide information regarding the bonding or antibonding between hybrids, while the latter can be used to quantify any inter-dimer repulsions.

Figure 1 illustrates the lowest frequency (207.04 cm^{-1}) buckling mode for the three-dimer cluster. Density matrices for the CASSCF LMOs were calculated along this mode. All off-diagonal density matrix elements (i.e., "bond orders") between LMOs on different Si-Si

dimers are calculated to be very small (< 0.01) along the entire buckling mode. This means that the buckling motion does not affect the bonding or antibonding dimer-dimer interactions.

The coulomb and exchange repulsion integrals were also calculated between the localized orbitals on different dimers along the same buckling mode (Fig. 1). As one would expect, the repulsions between two adjacent dimers decrease as the dimers buckle. For the three-dimer cluster, the total decrease in the total repulsion energy is 8.78 kcal/mol. So, the dimer-dimer repulsions do indeed favor buckling. Since the levels of theory employed here predict a symmetric (unbuckled) structure, factors other than inter-dimer repulsions must be dominant. It is likely that one such factor is the partial π interaction between two silicons in a dimer. Even though each dimer has a significant amount of diradical character (.35 electrons in the LUMO for each dimer pair), there is still some π bonding between these atom pairs. This bonding is likely to prefer the symmetric structure, even though Si-Si π bonding is much weaker than that between carbon atoms. Therefore, there appears to be two opposing forces affecting the structure of the dimer: The partial π bonding favors a symmetric dimer, while the repulsion prefers a buckled dimer. Since the CASSCF and MRMP2 single point potential energy surfaces predict that the symmetric dimers are the minimum energy structures, the dominant factor appears to be the partial π bond.

It is interesting that in many experiments the Si(100) surface is observed to be buckled.[6,7,24,25]. Based on their STM experiment,[27] Badt et al suggested that the buckling can be induced by a defect or a step at the surface. Recently, the dimer buckling at the S_A step of the clean Si(100) surface was studied using both STM techniques and theoretical methods.[30] Yokoyama et al.[31] conducted low temperature (63 K and 5 K) STM experiments and found that the dynamical flipping of the dimers are mostly frozen at 63 K leading to the $c(4\times2)$ reconstruction, whereas, when further cooled to 5 K, most dimers appear symmetric leading to $c(2\times1)$-like periodicity. With the 'flicker' noise detected in their STM images at 5 K, however, they concluded that the surface undergoes slow flip-flop motion of the buckled dimers during the STM scan at 5 K. Since the buckling modes have low frequencies (~200 cm^{-1}) and the calculations are done at 0 K, the experimental thermal conditions may leave the

system buckled upon cooling. It is also possible that the probe or a defect causes the buckling as the previous studies show.

Conclusion

The structure of the Si(100) surface was investigated using two-dimer ($Si_{15}H_{16}$) and three-dimer ($Si_{20}H_{21}$) surface cluster models. Because of the radical-like dangling bonds of the surface dimers, multi-reference wave functions were used to recover the quasi-degenerate non-dynamic electron correlation. CASSCF(4,4) and CASSCF(6,6) geometry optimizations for the two- and three-dimer clusters both generate only a symmetric structure as a minimum. This implies that dimer-dimer interactions do not play an important role in determining the structure of the surface. An analysis using CASSCF localized orbitals suggests that even though inter-dimer repulsions do decrease upon buckling, this effect is more than compensated by the preference of partial π bonding for the symmetric structure. The comparison of the dimer bond lengths for different cluster models shows that the dimer bond length is independent of cluster models as long as a proper multi-reference wave function is used. In order to further recover the dynamic part of the correlation, MRMP2 single point calculations were performed along the buckling normal modes. The MRMP2 results are consistent with the prediction of symmetric (or "unbuckled") structures.

Acknowledgment

This work was supported in part by a grant from the Air Force Office of Scientific Research. The calculations reported here were performed on an Alpha Cluster, obtained by grants from the Department of Energy and the National Science Foundation, and on the IBM SP2 at the Maui High Performance Computation Center through a DoD Grand Challenge grant. The authors thank Dr. Michael Schmidt for many helpful discussions.

References

1. C. J. Wu and E. A. Carter, Phys. Rev. B **45**, 9065 (1992)
2. W. A. Goddard III and T. C. McGill, J. Vac. Sci. Technol. **16**, 1308 (1979)
3. A. K. Rappe, T. A. Smedley, W. A. Goddard III, J. Phys. Chem. **85**, 1662 (1981)

4. P. Kratzer, B. Hammer, and J. K. Korskov, Phys. Rev. B **51**, 13432 (1993)
5. A. Vittandi, A. Selloni, and M. Casarin, Surf. Sci. **289**, 265 (1993)
6. H. Neergaard and J. T. Yates, Chem. Rev. **95**, 1589 (1995)
7. R. M. Tromp, R. J. Hamers, and H, E. Demuth, Phys. Rev. Lett. **55**, 1303 (1985); R. J. Hamers, Ph. Avouris, and F. Bozso *ibid.* **59**, 2071 (1987); R. J. Hamers, Rh. Avouris, and F. Bozso, J. Vac. Sci. Technol. A **6**, 508 (1988)
8. M. W. Schmidt, and M. S. Gordon, Annu. Rev. Phys. Chem. **49**, 233 (1998)
9. A. Redondo, and W. A. Goddard III, J. Vac. Sci. Technol. **21**, 344 (1982)
10. B. Paulus, Surf. Sci. **375**, 55 (1997)
11. J. Shoemaker, J. W. Burggraf, and M. S. Gordon, J. Chem. Phys. **112**, 2994 (2000)
12. M. S. Gordon, J. R. Shoemaker, and L. W. Burggraf, J. Chem. Phys. **113**, 9355 (2000)
13. J. S. Hess, and D. J. Doren, J. Chem. Phys. **113**, 9353 (2000)
14. R. Konecny, and D. J. Doren, J. Chem. Phys. **106**, 2426 (1997)
15. C. Yang, and H. C. Kang, J. Chem. Phys. **110**, 11029 (1999)
16. E. Penev, P. Kratzer, and M. Scheffler, J. Chem. Phys. **110**, 3986 (1999)
17. C. H. Choi, and M. S. Gordon, J. Am. Chem. Soc. **121**, 11311 (1999)
18. Y. Jung, C. H. Choi, and M. S. Gordon, J. Phys. Chem. B **105**, 4039 (2001)
19. P. J. Hay, and W. R. Wadt, J. Chem. Phys. **82**, 270 (1985); P. J. Hay, and W. R. Wadt, J. Chem. Phys. **82**, 284 (1985); P. J. Hay, and W. R. Wadt, J. Chem. Phys. **82**, 299 (1985)
20. M. W. Schmidt, K. K. Baldridge, J. A. Boatz, S. T. Elbert, M. S. Gordon, J. H. Jensen, S. Koseki, N. Matsunaga, K. A. Nguyen, S. Su, T. L. Windus, M. Dupuis, and J. A. Montgomery, Jr., J. Comput. Chem. **14**, 1347 (1993)
21. T. L. Windus, M. W. Schmidt, and M. S. Gordon, Theor. Chim. Acta **89**, 77 (1994)
22. Y. Alexeev, and M. S. Gordon (in preparation)
23. J. A. Steckel, T. Phung, K. D. Jordan, P. Nachtigall, J. Phys. Chem. B **105**, 4031 (2001)
24. R. A. Wolkow, Phys. Rev. Lett. **68**, 2636 (1992)
25. E. Pehlke, and M. Scheffler, Phys. Rev. Lett. **71**, 2338 (1993)
26. C. Yang, S. Y. Lee, H. C. Kang, J. Chem. Phys. **107**, 3295 (1997)
27. D. Badt, H. Wengelnik, H. Neddermeyer, J. Vac. Sci. Technol. B **12**, 2015 (1994)
28. W. J. Hehre, R. Ditchfield, and J. A. Pople, J. Chem. Phys. **56**, 2257 (1972); M. M. Francl, W. J. Pietro, W. J. Hehre, J. S. Binkley, M. S. Gordon, D. J. Defrees, and J. A. Pople, *ibid.* **77**, 3654 (1982)
29. Y. Wang, M. Shi, and J. W. Rabalais, Phys. Rev. B **48**, 1689 (1993)
30. H. Okada, T. Fujimoto, K. Endo, K. Hirose, and Y. Mori, Phys. Rev. B **63**, 195324 (2001)
31. T. Yokoyma, and K. Takayanagi, Phys. Rev. B **61**, R5078, (2000)
32. H. Nakano, J. Chem. Phys. **99**, 7983 (1993)
33. C. Edmiston, K.Ruedenberg, Rev. Mod. Phys. **35**, 457 (1963)
34. R. C. Raffenetti, K.Ruedenberg, C. L. Janssen, H. F. Schaefer, Theor. Chim. Acta **86**, 149 (1993)

Table 1. Dimer bond lengths of the reconstructed Si(100) surface.

Cluster model	Method	Length (A)	Reference
One-dimer (Si_9H_{12})	RHF/HW(d)	2.18	Shoemaker et al[a]
One-dimer (Si_9H_{12})	UHF/HW(d)[c]	2.32	This work
One-dimer (Si_9H_{12})	CASSCF(2,2)/6-31G(d)	2.28	Shoemaker et al[a]
One-dimer (Si_9H_{12})	CASSCF(2,2)/HW(d)	2.24	Shoemaker et al[a]
Two-dimer ($Si_{15}H_{16}$)	CASSCF(4,4)/6-31G(d)	2.28, 2.28	This work
Three-dimer ($Si_{20}H_{21}$)	CASSCF(6,6)/HW(d)	2.24, 2.25, 2.24	This work
Experiment	TOF-SARS	2.26 ±0.1	Wang et al[b]

[a] Reference 11

[b] Reference 29

[c] Severe spin contamination is observed, $\langle S^2 \rangle_{UHF} = 0.94$ ($\langle S^2 \rangle_{TRUE} = 0.00$ for a singlet state)

Table 2. Relative CASSCF and MRMP2 energies (kcal/mol) along the buckling normal modes.

	Buckling modes (cm^{-1})	Min[a]	5 %[b]	10 %[b]	15 %[b]	25 %[b]	50 %[b]	100 %[b]
			One-dimer (1 buckling mode)[c]					
TCSCF/6-31G(d)	191.34	0.00	0.04	0.15	0.33	0.93	3.68	14.06
MRMP2	191.34	0.00	0.02	0.10	0.21	0.60	2.40	10.08
			Two-dimer (2 Buckling modes)					
CASSCF(4,4)/6-	190.83	0.00	0.04	0.15	0.33	0.90	3.53	13.63
31G(d)	192.65	0.00	0.00	0.11	0.31	0.93	3.81	14.92
MRMP2	190.83	0.00	0.02	0.07	0.17	0.46	1.85	7.48
	192.65	0.00	0.00	0.06	0.17	0.52	2.17	8.93
			Three-dimer (3 Buckling Modes)					
CASSCF(6,6)/H	207.04	0.00	0.04	0.15	0.41	0.91	3.63	14.28
W(d)	207.26	0.00	0.04	0.17	0.38	1.05	4.18	16.38
	210.31	0.00	0.05	0.18	0.33	1.15	4.58	18.01
MRMP2	207.04	0.00	0.02	0.08	0.28	0.48	1.91	7.78
	207.26	0.00	0.03	0.11	0.24	0.67	2.68	10.96
	210.31	0.00	0.03	0.12	0.17	0.78	3.10	12.47

[a]Symmetric equilibrium structure.

[b]Degree of distortion from the equilibrium surface geometry along the buckling vibrational modes. For example, 100 % implies the geometry that corresponds to the maximum displacement along the buckling mode from the equilibrium structure.

[c]Previous study by Gordon et al. (reference 12)

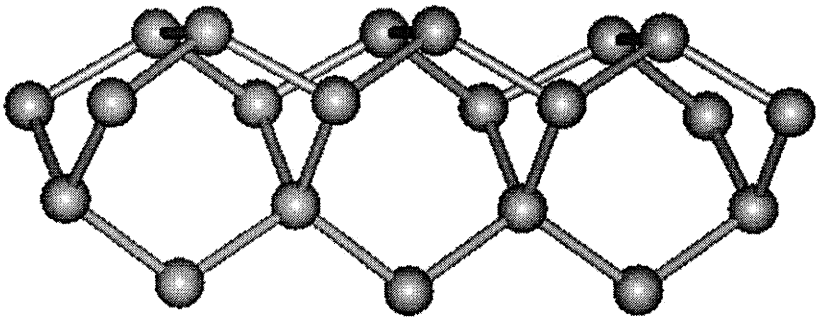

(a) Equilibrium structure

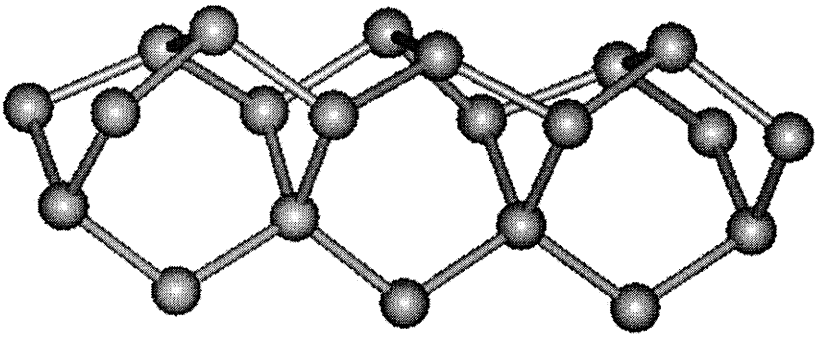

(b) Buckling mode (207.04 cm^{-1})

Figure 1. Structure of the three-dimer cluster

CHAPTER 3. ADSORPTION OF WATER ON THE Si(100) SURFACE: AN *AB INITIO* AND QM/MM CLUSTER STUDY

A paper published in *The Journal of Physical Chemistry B*[‡]

Yousung Jung, Cheol Ho Choi, and Mark S. Gordon

Abstract

The adsorption of water on the Si(100) surface is investigated using *ab initio* quantum chemical cluster calculations. A reaction profile is constructed using the MCSCF (multiconfigurational SCF) method. The calculations demonstrate that the reactant should be described with a multi-reference wave function in order to obtain correct energetics, because it contains a bare dimer with significant diradical character. The system becomes almost single configurational as water approaches the surface and forms a molecularly adsorbed intermediate. Therefore, except for the reactant, a single configurational wave function seems to be sufficient for a correct description of the reaction. The adsorbed OH group in an *isolated* product can nearly freely rotate between the trans and gauche minima. Interactions between the OH groups and the dangling bonds are small and do not appear to change the OH orientation. However, the interdimer hydrogen bonding is stronger and forces the OH orientation to be perpendicular to the dimer bond. The free rotation of the OH group in an *isolated* dimer model and the hydrogen bonding picture in an extended cluster model are consistent with the experimental finding for the OH orientation in the product. Si_9H_{12}, $Si_{15}H_{16}$, $Si_{32}H_{28}$, $Si_{48}H_{36}$ and $Si_{64}H_{44}$ cluster models for the Si(100) surface are used, and the SIMOMM (surface integrated molecular orbital molecular mechanics) method is used effectively for these large cluster calculations. The SIMOMM and full quantum results are compared.

[‡] *J. Phys. Chem. B* **105**, 4039-4044 (2001)

Introduction

Adsorption of water on the Si(100)-(2x1) surface has been studied extensively[1-5] due to its potential for applications to industry, such as growth of SiO_2 films by wet oxidation. Even though there has in the past been some controversy[5, 6] concerning whether water adsorbs molecularly or dissociatively on the Si(100) surface, dissociative adsorption now seems to be generally accepted as the most likely adsorption mechanism.[3, 7, 8] A recent theoretical study by Cho *et al.*[9], using the generalized gradient approximation (GGA) density functional theory (DFT) method and a slab model, is in agreement with this dissociative adsorption mechanism.

Besides the adsorption mechanism itself, structures of the products and interaction patterns among the products have also been of interest. ESDIAD studies[10, 11] and theoretical calculations[8, 9] suggest that OH groups are oriented normal to the silicon dimer bond. In their theoretical study, Konecny and Doren[8] used DFT cluster calculations to suggest that either hydrogen bonding between adjacent hydroxyls or dative-bond type interactions between an oxygen lone pair or hydroxyl hydrogen on one dimer and a dangling bond on an adjacent dimer in the same row is responsible for the orientation of the OH groups. Gurevich *et al.*[7] investigated these interaction patterns and the structures of the products using broadband infrared spectroscopy in combination with DFT cluster calculations. They concluded that "the water-exposed Si(100)-(2x1) surface is comprised of a mixture of single dimers with *isolated* hydroxyl groups and *paired* dimers that are coupled by hydrogen bonding between OH groups on neighboring dimers in the same row of the reconstructed 2x1 surface".

However, more recently Cho *et al.*[9] proposed that, although such hydrogen bonding or dative-bond type interactions may have a "profound" effect on the mechanism, the orientation of OH is 'insensitive' to such interactions by showing theoretically that the coverage of the surface with water has only a small effect on the Si-Si-O-H dihedral angle. Thus, there is some disagreement regarding the impact of hydrogen bonding or dative-bond type interactions on the OH orientation and it is one of the purposes of this work to investigate and hopefully provide some insight regarding this question.

The uppermost layer of the Si(100) surface is composed of dimers which have significant diradical character.[12-14] This makes the surface very reactive. Redondo and Goddard[15] first demonstrated that a silicon surface with singlet diradical dimers can be correctly described only with a multi-reference wave function. Many other papers[16-19] agreed with this notion, and more recently Paulus[20] and Shoemaker *et al.*[21] confirmed it again. Since the reactants of water/Si(100) also contain the bare surface, a multi-reference wave function is also required for a correct description of the adsorption reaction. In addition, since the adsorption reaction involves bond dissociation and formation, it is important to determine if key regions of the potential energy surface are single configurational or multiconfigurational in nature.

In this work, the potential energy surface is constructed using multi-reference wave functions to determine if the system is single configurational or multiconfigurational, by comparing the results with the results based on a single configurational wave function in terms of energetics and structural parameters. The structures of the products and the interactions among the products are considered in detail. The OH orientation with respect to the silicon dimer is discussed in relation to the interactions among the products. The results obtained from those calculations are compared with the experimental findings.

Recently, a new embedded cluster model, the surface integrated molecular orbital molecular mechanics (SIMOMM) method, has been developed for the study of surfaces.[22] SIMOMM can save considerable computational effort by representing many of the atoms with inexpensive MM potentials, while maintaining the quality of results. SIMOMM is also tested in this work for the water/Si(100) system, via comparison with the full quantum mechanical results.

Computational Details

The GAMESS electronic structure program was used for all calculations reported here. Recently, Shoemaker *et al.*[21] investigated basis set effects for surface clusters, and concluded that the Hay-Wadt effective core potential with its associated double zeta plus polarization valence basis set is a viable method for investigating the properties of large

clusters. In this work the Hay-Wadt effective core potential (ECP) plus polarization function basis set was used. This HW(d) basis set consists of double-zeta plus d polarization for the valence electrons and ECPs for the core electrons for Si. The 6-31G(d) basis[23] was employed for O and H. In order to assess the reliability of this mixed basis set, we also used two different all electron basis sets, DZV(d) consisting of the Dunning-Hay[24] double-zeta valence basis set plus d polarization functions and 6-31++G(d,p). Results obtained with the 6-31++G(d,p) basis set are directly compared to the previous DFT/B3LYP/6-31++G(d,p) study in Table 1.

Since the reactant includes the bare surface with dangling bonds, the generalized valence bond (GVB) or two configuration SCF (TCSCF) method was employed. Since the natural orbital analysis revealed that the occupation number for the virtual orbital in the active space was small (≤ 0.04) except for the reactant (see below), Hartree-Fock (HF) wave functions were used for the rest of the calculations (except for direct comparisons with reactant), particularly for the study of product structures. However, clusters containing a bare surface were always treated with the GVB wave functions.

For the minimum energy reaction path, all stationary points were identified as minima or transition states by computing and diagonalizing the Hessian matrix. A first order saddle point (transition state) was characterized by one imaginary frequency from the Hessian diagonalization and a minimum by no imaginary frequency. The intrinsic reaction coordinate (IRC), using the Gonzalez-Schlegel second-order method[25], was used to connect the minimum energy reaction path with a step size of 0.30 $amu^{1/2}$ bohr. To recover the dynamic electron correlation, the energies at all stationary points at the RHF level of theory were recalculated with the Møller-Plesset second-order perturbation method[26], denoted MP2//RHF. Similarly, multi-reference second-order perturbation theory was used to augment the TCSCF multi-reference wave functions. The MCQDPT2 method (multiconfigurational quasi-degenerate second-order perturbation theory)[27] was used in the present work. The notation MCQDPT2//TCSCF means that a single point energy correction was performed with the MCQDPT2 method at a TCSCF (equivalent o GVB-PP(1)) optimized geometry.

Si_9H_{12}, $Si_{15}H_{16}$, $Si_{32}H_{28}$, $Si_{48}H_{36}$ and $Si_{64}H_{44}$ cluster models (Fig 1) for the Si(100) surface were employed in this work. For the dissociative adsorption mechanism, a

Si_9H_{12}/H_2O cluster model was used, and SIMOMM and full quantum results were compared. For the study of the interaction patterns and the structures of the product, Si_9H_{12}/ H_2O, $Si_{32}H_{28}/ H_2O$, $Si_{15}H_{16}/2H_2O$, $Si_{32}H_{28}/2H_2O$, $Si_{48}H_{36}/3H_2O$ and $Si_{64}H_{44}/4H_2O$ SIMOMM models were used. The waters are always treated with *ab initio* wave functions.

Results and Discussion

A. Adsorption mechanism of H_2O within the single dimer cluster model. The potential energy surface for the dissociative adsorption of water on the Si(100) surface, based on the Si_9H_{12} cluster model, is depicted in Fig 2. Water adsorbs dissociatively on the Si(100) surface with a small *net* reaction barrier. Table 1 summarizes the relative energies along the minimum energy path.

First consider basis set effects on the energetics in Table 1. There are large differences between HW(d) and all electron relative energies, while the two all electron basis sets, DZV(d) and 6-31++G(d,p), give very similar results to each other. However, the mixed basis set improves the results significantly, with relative energies that are nearly the same as those obtained with the all electron basis sets. These results suggest that HW(d) is a reliable and effective basis set for the silicon surface itself, while a better basis set is necessary for the lighter elements.

As can be seen in Table 1, except for the reactant, single configuration (i.e., RHF, MP2) energetics are in excellent agreement with the multi-reference (i.e., GVB, MCQDPT2) results for the same basis sets and analogous levels of theory. RHF structural parameters (Table 2) are also in nearly perfect agreement with the GVB-PP(1) structural parameters except for the reactant. The same calculations were performed with the same cluster model (Si_9H_{12}) using the SIMOMM method in which the water molecule and the first two top surface layers, a dimer layer and the layer directly connected to the dimer layer, were treated quantum mechanically and the rest of the cluster was treated classically. In Fig 1, the colored atoms were treated with quantum mechanics and the gray ones with molecular mechanics. The full QM and SIMOMM methods with the Si_9H_{12} cluster model give almost the same results, for the same basis sets, wave functions (RHF or GVB-PP(1)) and levels of theory.

The only significant differences between GVB-PP(1) and RHF results occur in the reactant. Since the reactant includes the bare surface with significant diradical character, it is natural that a difference between the single configurational and multiconfigurational methods exists for this structure. Since RHF gives essentially the same results as GVB-PP(1) along the reaction path, except for the reactant, in terms of the energetics and the structural parameters, it appears that the whole reaction path except the reactant can be described by single configurational wave functions. We conclude from these calculations that the bare surface loses its singlet diradical character as water approaches the surface and the system becomes single configurational when water undergoes weak molecular adsorption onto the surface.

Natural orbital occupation numbers from the GVB-PP(1) calculation at each critical point are listed in Table 3. Occupation numbers for the antibonding LUMO orbital at all stationary points except the reactant are very small. So the contribution of this virtual orbital is not important at these points. Again, this suggests that the system is single configurational. It is therefore likely that a GVB-PP(1) wave function is sufficient for the exploration of the entire reaction path, and that a RHF-based wave function is sufficient if one is interested only in the intermediate, the transition state and the product.

The energetics in Table 1 also show that MCQDPT2//GVB-PP(1) results are in reasonably good agreement with previous DFT studies[8, 9] with the same basis set except for the reactant. The only significant difference is the extent to which the intermediate is stabilized relative to the reactant. The difference is considered to be due to the inadequate treatment of the diradical character in the reactant by the DFT method. This also impacts the predicted sign of the overall reaction barrier. The MCQDTP2//GVB-PP(1) energetics predict a *net* reaction barrier of ~4 kcal/mol with the 6-31++G(d,p) basis, while DFT predicts no *net* reaction barrier. In any event, the small overall reaction barrier implies that water can be adsorbed on the Si(100) surface fairly easily, even with small thermal fluctuations. This is consistent with the experimental observation of the high sticking coefficient for the adsorption reaction.[1]

The previous DFT study predicted a transition state with the OH group pointing gauche (~60°) with respect to the silicon dimer. However, in the present calculations, all trial

geometries for the gauche (~60°) transition state converged to the gauche' (~130°) form, even though product structures with the OH oriented gauche (~60°) as well as trans (~180°) with respect to the silicon dimer were found. Therefore, the isomerization reaction between the trans (~180°) and gauche (~60°) product structures was explored. A Si_9H_{12} full QM cluster study (Table 4) shows that the thermodynamic stability for the product is nearly independent of rotation angle, and the reaction barrier for the isomerization is very small. This implies free rotation of the OH group on the surface. The experimentally determined orientation of OH is perpendicular to the silicon dimer, neither gauche nor trans. So if the OH group rotates freely, then the experimentally measured value would be the average of the two theoretically possible structures.

It is also possible that the potential energy surface bifurcates at the transition state to produce both trans (~180°) and gauche (~60°) products from one gauche' (~130°) transition state. If the PES bifurcates, this bifurcation would very likely be coupled to free rotation of the OH group. More detailed discussion about the OH orientation and the isomerization of the product is given in the next section.

B. OH orientation and interaction patterns among the products. Next consider the interaction patterns among the products and the effect of these interactions on the OH orientation using extended cluster models. These discussions are based on SIMOMM RHF calculations since, as discussed in the previous section, SIMOMM is very reliable for this system and the RHF level of theory is also sufficient for a correct description of the product. However the cluster models including the bare surface dimer were treated with the GVB-PP(1) wave function. Second-order perturbation theory single point energy calculations, MP2//RHF or MCQDPT2//TCSCF, were performed at the RHF or GVB geometries for more accurate energetics.

In order to investigate the interactions between the hydroxyl hydrogen or oxygen lone pair and silicon dangling bonds, the $Si_{32}H_{28}$ two-dimer cluster model ((c) in Fig 1) was employed. One side of the two-dimer model is saturated with OH and H groups and the other

is exposed as a bare surface (dangling bonds). Because of the dangling bonds on one side, the GVB-PP(1) wave function was used.

In Table 4, we compare the torsion angle of the OH group, the buckling angle and the rotational barrier between the gauche and trans forms. Increasing the cluster size from the single dimer to the two-dimer cluster model does not have any effect on the torsion angle of the OH group with respect to the silicon dimer. The buckling angles for both dimers in the two-dimer model are also still ~zero suggesting that the dangling bonds and the OH group do not interact strongly, while the previous DFT study[8] predicted more than 10° of buckling for one dimer and zero for the other. In addition, there is no significant change in the rotational barrier from the gauche to the trans form. If there was significant attractive interaction between the OH group and the dangling bonds, one would expect an increase in potential barrier for the rotation. Therefore, it is concluded that the dangling bonds do not interact with the OH group and do not change the orientation of the OH group. These results are probably due to the long distance between the two dimers in the reconstructed Si(100)-(2x1) surface. In contrast, in the previous study[8], the OH orientation increased from 56° to 84°, apparently as a result of dative-bond type interactions with the increase of cluster size.

In order to examine hydrogen bonding patterns for the hydrolyzed Si(100) surface, SIMOMM calculations were performed with two, three and four dimer cluster models ((c), (d) and (e) in Fig 1), with all the dangling bonds saturated with OH and H. Table 5 summarizes hydrogen bond distances and Si-Si-O-H torsion angles. The electron correlated method, MP2/HW(d), produces shorter hydrogen bond distances between (O)H and O(H) than the Hartree-Fock method. Consequently, the O··H bond orders at the MP2 geometries are larger. This suggests that electron correlation effects play an important role in hydrogen bond formation. In order to examine the basis set effect on the hydrogen bonding patterns, the DZV(d) basis set was employed for the $Si_{32}H_{28}/2H_2O$ cluster model. This better basis set produces a somewhat weaker hydrogen bond (2.32 Å O··H) than the HW(d) basis (1.96 Å O··H). It is likely the larger basis set will also result in slightly weaker hydrogen bonds in the three and four dimer cluster models. The comparison of MP2/DZV(d) and RHF/DZV(d)

optimized hydrogen bond distances also indicates that the MP2 method predicts stronger hydrogen bonds.

MP2/HW(d) optimized structures showing hydrogen bonding patterns are depicted in Fig 3. As noted earlier, in an *isolated* dimer product (single dimer model) the free rotation between gauche (60°) and trans (180°) forms of the product or the bifurcation of the potential energy surface would lead to a rotation angle similar to the experimentally determined OH orientation with respect to silicon dimer (~90°). However, if the dimer adjacent to this *isolated* product is also saturated with OH and H, then free rotation is no longer possible and the trans form is no longer a local minimum. Now, the minimum energy structure is the one in which two adjacent hydroxyls form a hydrogen bond (Fig 3). Because of the formation of hydrogen bonds, the OH orientation with respect to the Si dimer converges to about 85°, not the gauche (60°) or trans (180°) angles found in *isolated* products. Thus, when OH and H saturate the surface there is apparently only one structure, in which OH is oriented normal to the silicon dimer bond due to hydrogen bond formation. Still, in this hydrogen bonding picture, dimer buckling is not observed. This agrees with the previous DFT study.[8]

In their IR study, Gurevich *et al.*[7] proposed that hydroxyl-mediated interdimer coupling does not extend to the second adjacent dimer (no consecutive hydrogen bonds in the same row) based on the fact that there was no further shift of OH stretch frequency as the coverage was increased. As can be seen in Fig 3, our calculations also show that hydrogen bonding occurs only within the adjacent hydroxyls and does not propagate further. This appears to be due to the long distance between two adjacent dimers in the same row. Because of the long distance, in order to form a hydrogen bond, one OH group is tilted forward and the other OH is tilted backward, and this pattern makes the extension of hydrogen bonding difficult.

Conclusions

Adsorption of water on the Si(100) surface was studied by fully quantum mechanical calculations and the hybrid QM/MM SIMOMM method. Comparison of full QM calculations and SIMOMM calculations show that the computationally efficient SIMOMM method gives

reasonable results. It is shown that an all electron basis set is required for the water molecule, whereas an effective core potential basis augmented with polarization functions is sufficient and effective for the surface itself. Therefore, it is proposed that the mixed basis set, consisting of all electron basis for the target molecule and effective core potential plus polarization functions basis for the silicon surface itself, can be used effectively for the study of various chemical reactions on the Si(100) surface.[28]

The potential energy surface for the adsorption of water on Si(100), modeled with the Si_9H_{12} cluster, was constructed. Because the reactant has significant singlet diradical character, multi-reference wave functions were used for the correct description of the entire potential energy surface. Calculations with GVB-PP(1)/6-31++G(d,p) followed by MCQDPT2//TCSCF/6-31++G(d,p) energy correction reveal that there is a *net* reaction barrier of ~4 kcal/mol. This small reaction barrier is consistent with the experimentally determined high sticking coefficient. A natural orbital occupation number analysis and comparison of GVB-PP(1) results with RHF illustrate that the entire reaction path, except for the diradicaloid reactant, is actually single configurational, even though the reaction involves bond dissociation and formation processes.

Two possible structures for an *isolated* product were found, having gauche or trans orientation of the OH group with respect to the silicon dimer. Both the rotational barrier and the energy difference between these two forms were calculated to be small in a single dimer cluster model. This suggests that the experimentally determined OH orientation in an *isolated* product, normal to the dimer bond, is actually an averaged orientation of the gauche (60°) and trans (180°) forms.

Extended cluster model calculations were performed to identify the interaction patterns responsible for the OH orientation of the product with respect to the dimer bond. Calculations with *isolated* two-dimer cluster models indicate that the dangling bonds next to the dimer in the same row saturated with OH and H do not have any effect on free rotation of the OH group and do not change the OH orientation. However, when two consecutive dimers are saturated simultaneously with OH and H, a hydrogen bond between these two OH groups is formed. Due to this hydrogen bonding, the trans minimum vanishes and the Si-Si-O-H

torsion angle changes to around 85°, close to the experimental observation (~90°). Therefore, we conclude that there is no interaction between hydroxyl groups (oxygen lone pair or the hydroxyl hydrogen) and the dangling bonds, probably because of the long distance between the two neighboring dimers, and that there is a hydrogen bonding interaction between two adjacent hydroxyl groups in the same row. The latter interaction changes the OH orientation to be nearly perpendicular to the dimer bond. This resolves the question regarding the relative importance of hydrogen bonding vs. dative-bond type interactions on the product configuration (the OH orientation with respect to the dimer bond).

The computations presented here with three and four dimer cluster models demonstrate that the interdimer hydrogen bonding occurs only between two adjacent dimers, as originally proposed by Gurevich *et al.*[7] based on their experimental observation, rather than extended to the hydrogen bonding network. Electron correlation appears to be very important for an accurate description of hydrogen bond.

Acknowledgment

This work was supported in part by a grant from the Air Force Office of Scientific Research. The calculations described here were performed on an IBM Power3 Cluster, obtained by grants from IBM and the Department of Energy, administered by the Ames Laboratory.

References and Notes

1. Chabal, Y. J.; Christman, S. B. *Phys. Rev. B* **1984**, 29, 6974.
2. Irene, E. A. *Electrochem. Soc.* **1978**, 125, 1708.
3. Raghavachari, K.; Chabal, Y. J.; Struck, L. M. *Chem. Phys. Lett.* **1996**, 252, 230.
4. Schaefer, J. A.; Gopel, W. *Surf. Sci.* **1985**, 155, 535.
5. Thiel, P. A.; Madey, T. E. *Surf. Sci. Rept.* 1987, 7, 211.
6. Waltenberg, H. N.; J.T. Yates, J. T. Jr. *Chem. Rev.* **1995**, 95, 1589.
7. Gurevich, A. B.; Stefanov, B. B.; Weldon, M. K.; Chabal, Y. J.; Raghavachari, K. *Phys. Rev. B* **1998**, 58, 13434.
8. Konecny, R.; D.J. Doren, D. J. *J. Chem. Phys.* **1997**, 106, 2426.
9. Cho, J. H.; Kim, K. S.; Lee, S. H.; Kang, M. H. *Phys. Rev. B* **2000**, 61, 4503.
10. Gao, Q.; Dohnalek, Z.; Cheng, C. C.; Choyke, W. J.; Yates, J. T. Jr. *Surf. Sci.* **1994**, 312, 261.

11. Larsson, C. U. S.; Flodstrom, A. S.; Nyholm, R.; Incoccia, L.; Senf, F. *J. Vac. Sci. Technol. A* **1987**, 5, 842.
12. Appelbaum, J. A.; Baraff, G. A.; Gamann, D. R. *Phys. Rev. B* **1976**, 14, 588.
13. Hamers, R. J.; Tromp, R. M.; Demuth, J. E. *Phys. Rev. B* **1986**, 34, 5343.
14. Radeke, M. R.; Carter, E. A. *Annu. Rev. Phys. Chem.* **1997**, 48, 243.
15. Redondo, A.; Goddard, W. A. *J. Vac. Sci. Technol.* **1982**, 21, 344.
16. Nachtigall, P.; Jordan, K. D.; Janda, K. C. *J. Chem. Phys.* **1991**, 95, 8652
17. Wu, C. J.; Carter, E. A. *Phys. Rev. B* **1992**, 45, 9065.
18. Jing, Z.; Whitten, J. L. *Surf. Sci.* **1992**, 274, 106
19. Jing, Z.; Whitten, J. L. *J. Chem. Phys.* **1995**, 102, 3867
20. Paulus, B. *Surf. Sci.* **1998**, 408, 195.
21. Shoemaker, J. R.; Burgraff, L. W.; Gordon, M. S. *J. Chem. Phys.* **2000**, 112, 2994. Gordon, M. S; Shoemaker, J. R.; Burggraf, L. W. *J. Chem. Phys.*, in press
22. Shoemaker, J. R.; Burgraff, L. W.; Gordon, M. S. *J. Phys. Chem. A* **1999**,103, 3245.
23. Hariharan, P. C.; Pople, J. A. *Theoret. Chim. Acta* **1973**, 28, 213.
24. Dunning, T. H.; Hay, P. J. In *Methods of Electronic Structure Theory.*
25. Gonzalez, C.; Schlegel, H. B. *J. Phys. Chem.* **1990**, 94, 5523.
26. Pople, J. A; Binkley, J. S.; Seeger, R. *Int. J. Quantum Chem.* **1976**, 10, 1
27. Nakano, H. *J. Chem. Phys.* **1993**, 99, 7983.
28. This mixed basis set, consisting of HW(d) for the surface and 6-31G(d) for cyclopentadiene, worked very well in the study of cycloaddition reaction of cyclopentadiene on the Si(100) surface recently performed in our group. The results with the mixed basis set were in good agreement with the DZV(d) all electron basis results.

Table 1. Relative energies of the structures along the minimum reaction path

	Reactant	Intermediate	TS	Product
	Full QM			
RHF/HW(d)	35.5	0	6.9	-63.7
MP2//RHF/HW(d)	33.0	0	2.4	-52.5
GVB-PP(1)/HW(d)	22.1	0	6.2	-65.7
MCQDPT2//TCSCF/HW(d)	27.0	0	3.0	-53.6
RHF/MIXED[b]	14.5	0	13.1	-66.3
MP2//RHF/MIXED[b]	12.7	0	5.6	-54.2
GVB-PP(1)/MIXED[b]	1.3	0	12.3	-68.0
MCQDPT2//TCSCF/MIXED[b]	6.9	0	6.4	-55.0
RHF/DZV(d)	15.2	0	15.9	-60.4
MP2//RHF/DZV(d)	10.2	0	7.4	-49.0
GVB-PP(1)/DZV(d)	2.5	0	14.7	-62.7
MCQDPT2//TCSCF/DZV(d)	5.8	0	8.4	-49.9
RHF/6-31++G(d,p)	13.4	0	15.2	-58.2
MP2//RHF/6-31++G(d,p)	8.2	0	7.2	-46.5
GVB-PP(1)/6-31++G(d,p)	0.9	0	14.0	-60.2
MCQDPT2//TCSCF/6-31++G(d,p)	4.3	0	8.5	-46.8
	SIMOMM			
RHF/HW(d)	32.4	0	7.1	-65.6
MP2//RHF/HW(d)	31.0	0	2.3	-55.6
GVB-PP(1)/HW(d)	17.9	0	6.5	67.4
MCQDPT2//TCSCF/HW(d)	24.1	0	3.1	-55.9
RHF/MIXED[b]	11.5	0	13.2	-68.5
MP2//RHF/MIXED[b]	10.9	0	5.6	-57.7
GVB-PP(1)/MIXED[b]	1.9	0	12.7	-69.8
MCQDPT2//TCSCF/MIXED[b]	4.2	0	6.6	-57.7
B3LYP/6-31++G(d,p)[a]	14.1	0	7.0	-44.4
B3LYP/6-311G(d,p)[a]	12.9	0	1.6	-49.9
B3LYP/6-311++G(2df,2p)[a]	7.2	0	1.1	-51.8

[a] previous DFT study by Konecny *et al.* (reference 8)

[b] mixed basis set: HW(d) for Si and 6-31G(d) for H and O

Table 2. Important structural parameters along the minimum reaction path

	Si-Si at reactant	Si-O at intermediate	Si-Si-O-H at TS	Si-O at product	Si-Si-O-H at product
		Full QM			
RHF/HW(d)	2.151	1.864	180.0	1.651 (1.651)	179.0 (59.1)
GVB-PP(1)/HW(d)	2.241	1.867	180.0	1.651 (1.651)	179.9 (60.2)
RHF/MIXED[a]	2.151	1.959	126.7	1.652 (1.652)	179.9 (60.5)
GVB-PP(1)/MIXED[a]	2.241	1.972	125.5	1.652 (1.652)	179.0 (60.8)
RHF/DZV(d)	2.185	1.975	137.9	1.659 (1.659)	179.9 (59.8)
GVB-PP(1)/DZV(d)	2.278	1.984	135.0	1.659 (1.659)	179.4 (60.3)
RHF/6-31++G(d,p)	2.189	1.993	135.9	1.670 (1.670)	179.9 (59.9)
GVB-PP(1)/6-31++G(d,p)	2.278	2.003	133.1	1.671 (1.670)	178.2 (61.7)
		SIMOMM			
RHF/HW(d)	2.154	1.863	180.0	1.651 (1.651)	179.7 (57.0)
GVB-PP(1)/HW(d)	2.243	1.869	180.0	1.651 (1.651)	180.0 (57.3)
RHF/MIXED[a]	2.154	1.964	126.0	1.653 (1.653)	179.9 (57.2)
GVB-PP(1)/MIXED[a]	2.243	1.993	124.5	1.653 (1.653)	178.4 (58.5)
BLYP/TZ94P[b]	2.227	2.231	59.0	1.757	62.2

[a]mixed basis set: HW(d) for Si and 6-31G(d) for H and O
[b]previous DFT study by Konecny *et al.* (reference 8)

Table 3. Natural orbital occupation numbers at critical points along the minimum reaction path

		Reactant	Intermediate	TS	Product
		Full QM			
GVB-PP(1)/HW(d)	Bonding	1.63	1.96	1.96	1.98
	Antibonding	0.37	0.04	0.04	0.02
GVB-PP(1)/DZV(d)	Bonding	1.68	1.96	1.96	1.98
	Antibonding	0.32	0.04	0.04	0.02
		SIMOMM			
GVB-PP(1)/HW(d)	Bonding	1.68	1.96	1.96	1.98
	Antibonding	0.32	0.04	0.04	0.02

Table 4. Rotational barrier for the isomerization and the buckling angle in an *isolated* product; E is the energy difference and E_b is the rotational barrier for the isomerization reaction from the trans to the gauche form

	E_b (kcal/mol)	E (kcal/mol)	Si-Si-O-H (°)	Buckling angle(°)
Full QM (Si_9H_{12}/H_2O)				
MP2//RHF/HW(d)	0.6	-0.3	59.1, 179.0	
MP2//RHF/DZV(d)	0.5	-0.4	59.8, 179.9	
BLYP/TZ94P[a]			62.2	
SIMOMM ($Si_{32}H_{28}/H_2O$)				
MCQDPT2//GVB-	0.2	-1.6	57.7, 176.7	No buckling, No buckling
PP(1)/HW(d)	0.4	-1.3	-57.1, -177.0	No buckling, No buckling
MCQDPT2//GVB-	0.6	-1.0	56.4, 178.0	No buckling, No buckling
PP(1)/DZV(d)	0.8	-0.9	-56.2, -178.0	No buckling, No buckling
DFT ($Si_{15}H_{16}/H_2O$)				
BLYP/TZ94P[a]			84.5	12.7, No buckling
			-81.8	11.4, No buckling

[a]previous DFT study by Konecny *et al.* (reference 8)

Table 5. Selected geometric parameters in the hydrogen bonding picture, Fig 3. Values are from MP2/HW(d) optimized structures; in parenthesis are from RHF/HW(d) geometries

	(H)O···H(O) (Å)	(H)O···H(O) RHF Bond order	Si-Si-O-H (°)
(a) $Si_{15}H_{16}/2H_2O$	1.90 (2.18)	0.10 (0.06)	83.9 (85.6)
			68.0 (69.0)
(b) $Si_{32}H_{28}/2H_2O$	1.96 (2.30)	0.09 (0.05)	83.0 (84.8)
			68.8 (70.7)
(c) $Si_{48}H_{36}/3H_2O$	2.08 (2.48)	0.08 (< 0.05)	84.1 (83.7)
	3.04 (3.25)		80.4 (81.8)
			66.8 (67.6)
(d) $Si_{64}H_{44}/4H_2O$	1.97 (2.34)	0.09 (< 0.05)	83.2 (84.8)
	3.93 (3.83)		73.2 (76.7)
	1.99 (2.39)	0.09 (< 0.05)	83.9 (86.1)
			68.9 (70.1)
(e) $Si_{32}H_{28}/2H_2O$[a]	2.32 (2.91)[a]	< 0.05 (< 0.05)[a]	82.5 (80.5)[a]
			63.8 (63.6)[a]

[a]DZV(d) basis set is used.

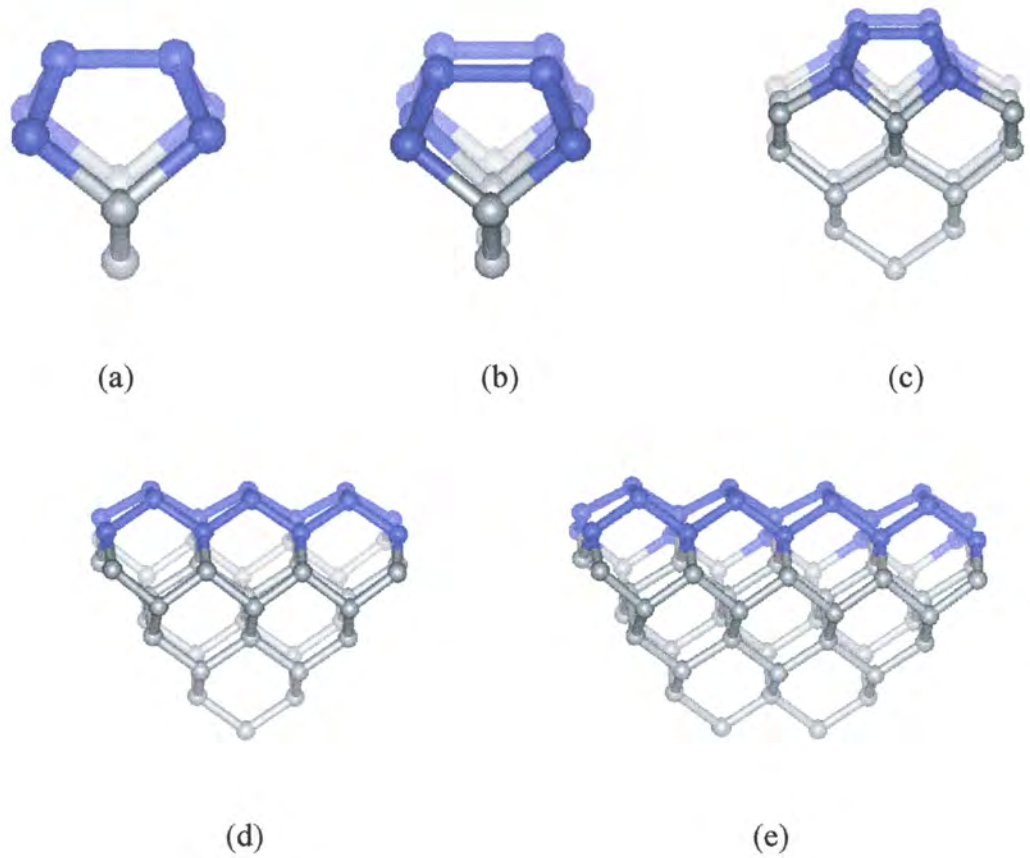

Figure 1. Cluster models used in this study: (a) Si_9H_{12} (b) $Si_{15}H_{16}$ (c) $Si_{32}H_{28}$ (d) $Si_{48}H_{36}$ (e) $Si_{64}H_{44}$. The colored atoms are treated quantum mechanically and the gray ones molecular mechanically.

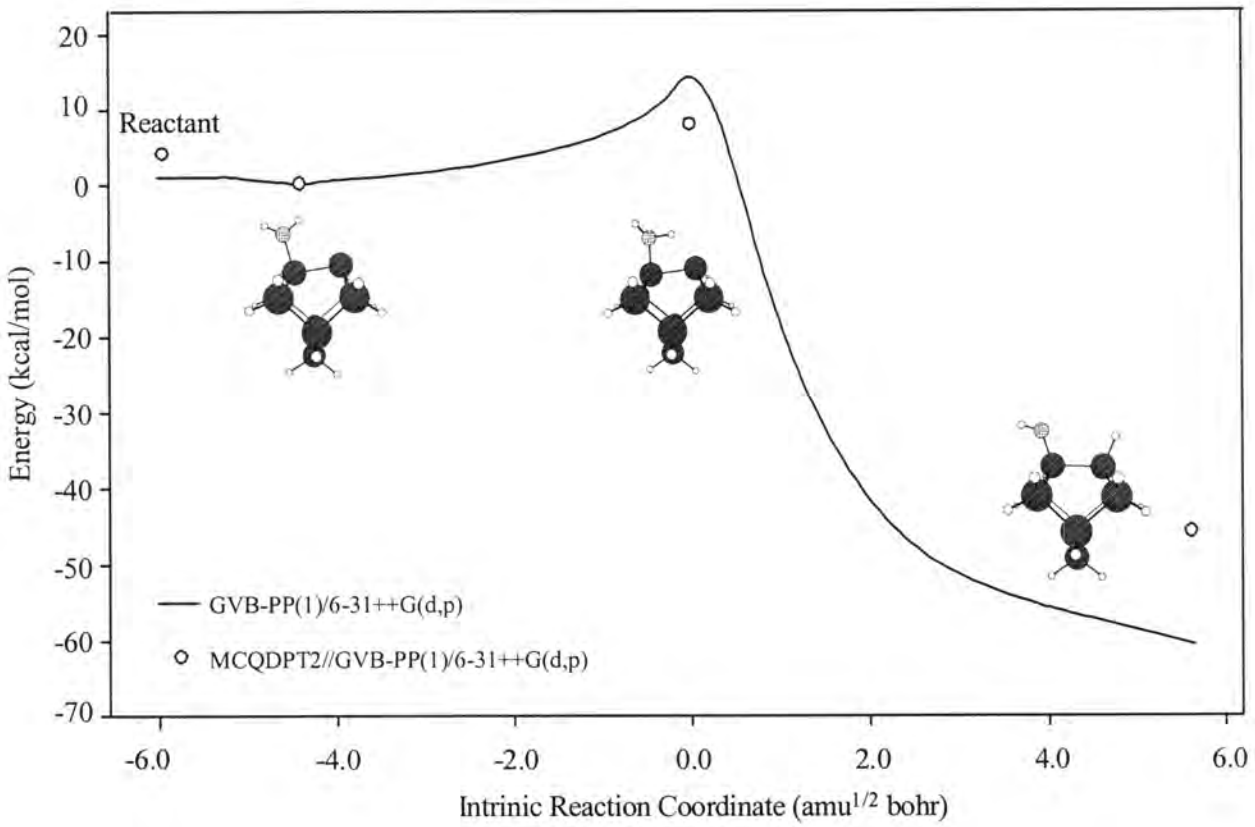

Figure2. The potential energy surface for the dissociative adsorption of water on the Si(100) surface. Intrinsic reaction coordinate (IRC) calculations connect the intermediate, the transition state, and the product. The data point at reactant is from geometry optimization.

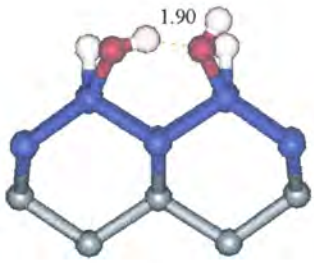

(a) $Si_{15}H_{16}/2H_2O$

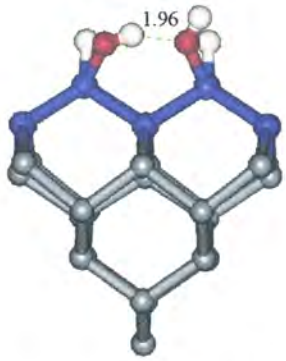

(b) $Si_{32}H_{28}/2H_2O$

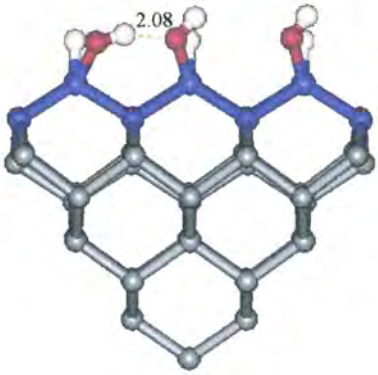

(c) $Si_{48}H_{36}/3H_2O$

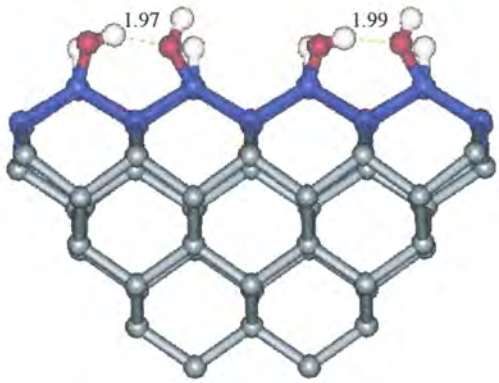

(d) $Si_{64}H_{44}/4H_2O$

Figure 3. Hydrogen bonding patterns among the adsorption products. The silicon atoms in blue and the OH and H fragments from the water molecule are treated with quantum mechanics and the others with molecular mechanics.

CHAPTER 4. CYCLOADDITION OF BENZENE ON Si(100) AND ITS SURFACE CONVERSIONS

A paper to be submitted to Main Group Chemistry

Yousung Jung and Mark S. Gordon

Abstract

A comprehensive *ab initio* study of adsorption of benzene on the silicon (100) surface is presented. Five potential candidates for the reaction product are examined to determine the lowest energy adsorption configuration. A [4+2]-like structure, **2**, is determined to be the global minimum, although a tetra-σ bonded structure, **3**, is very similar in energy to **2**. Multi-reference perturbation theory suggests that the [4+2]-like addition of benzene on Si(100) is very similar to the barrierless Diels-Alder reaction even though benzene adsorption entails the loss of benzene aromaticity during reaction. The calculations demonstrate that the [2+2] cycloaddition can also occur if the reaction follows a non-symmetric pathway. Large occupation numbers for the active anti-bonding orbitals used in the CASSCF(10,10) calculations illustrate the importance of using multi-reference wave functions for a correct description of this system.

Introduction

Organic modification of semiconductor surfaces is becoming very popular due to its industrial importance for the developments of new functional surfaces and molecular scale electronics. Such surfaces, modified with organic molecules, can attain additional useful properties such as optical activity and bio-functionality. For example recently, Lopinski et al showed that a chiral surface can be prepared by introducing 1S(+)-3-carene onto the silicon (100) surface.[1]

In addition, introducing hydrocarbons onto the Si(100) surface is a potentially important process for SiC film growth. Studies on ethylene and acetylene on Si(100) have shown that C-C π bonds in alkenes or alkynes can readily react with the dangling bonds of the surface dimer of the reconstructed Si(100) surface.[2-9] The carbons in these unsaturated

hydrocarbons undergo rehybridization to form Si-C σ bonds with the silicon surface dimers. The adsorption product is thereby similar to the [2+2] four-membered ring cycloaddition adduct. While the adsorption of many unsaturated hydrocarbons on Si(100) is essentially irreversible, previous thermal desorption experiments showed that benzene adsorbs and desorbs almost "reversibly" on the Si(100) surface.[10]

Taguchi et al used TDS, EELS, LEED, and AES spectroscopic tools and demonstrated that benzene is chemisorbed non-dissociatively on the silicon surface both at 90 and 300 K.[10] Chemisorbed benzene was observed to have both sp^2 and sp^3 hybridized carbon atoms. They estimated the fractional saturation coverage of benzene on Si(100) to be ~0.27 ML which corresponds to one benzene molecule per two surface silicon dimers (1 ML means one target molecule per surface atom). Based on their experimental data, they proposed two possible candidates for the adsorption product, **1** and **2** in Chart1. Structure **1** corresponds to a [2+2] cycloaddition product and **2** to a [4+2] product.

Theoretical results for the adsorption structures of benzene on Si(100) were first presented by Craig using the SLAB-MINDO semi-empirical method.[11] A number of possible product configurations were compared, and [2+2]-like products (**1** and **6**) were suggested as preferred structures. Other semi-empirical calculations by Jeong et al[12] followed. The PM3 semi-empirical method with a $Si_{43}H_{32}$ four-layer cluster model was used, and a symmetric radical-like structure, **5**, was predicted to be the most stable adsorption product. However, in their calculations, several geometric constraints were imposed on the surface structure. This is particularly inappropriate because the surface dimer with partial double bond character will be rehybridized into a fully single bond during the surface reaction, but those structural constraints on the surface dimer certainly cannot describe this phenomenon correctly.

A combined experimental and theoretical study of the adsorption of benzene on Si(100) was conducted by Gokhale et al.[13,14] Angle-resolved photoemission spectra suggested that the reaction product should have local C_{2v} symmetry with the molecular plane parallel to the surface dimer. Based on this local C_{2v} symmetry argument, two possible structures were predicted, the [4+2] and symmetric radical-like structures (**2** and **5**). Their DFT calculations with $Si_{15}H_{16}$ and $Si_{13}H_{13}$ cluster models further suggested that **2** is energetically the most stable product.

On the other hand, the STM experiments by Lopinski et al suggested three different configurations for the reaction product:[15-17] one corresponding to a di-σ bonded geometry on-top of a single dimer, and two corresponding to a tetra-σ bonded geometry arranged over two dimers. Their STM images as a function of time also indicated that, while a single dimer state (di-σ bonded structure) was populated preferentially upon adsorption, it was converted to a tetra-σ bonded structure bridging two dimers on a longer timescale. This suggests that the single dimer geometry is metastable. The activation barrier for this conversion was estimated to be 0.95 eV (22 kcal/mol). The comparison of the real STM images with the simulated ones (by the calculation of charge density iso-surfaces of occupied valence states) verified that **2** is the metastable single dimer state, and **3** and **4** are the two final bridge states. Their DFT//HF calculations (B3LYP/6-31G(d) single point energy correction after geometry optimization with HF/3-21G(d)) further suggested that **3** is the global minimum.

Conversion of the adsorption products was also suggested by Borovsky et al using STM techniques.[18] They found that the metastable species is symmetric, and that the final state to which the metastable species converts is located over two surface dimers. Based on these findings, they proposed that **2** is metastable and **1** is the final state. The activation barrier for this conversion was predicted to be about 23 kcal/mol assuming a prefactor of 10^{13} Hz. Although this conversion barrier is similar to the one previously suggested by Lopinski et al, it should be noted that the types of conversion are different from each other: one is from **2** to **1** and the other is from **2** to **3** (or **4**).

Another experimental study using vibrational IR spectroscopy, thermal desorption and near-edge X-ray absorption fine structure (NEXAFS) showed that benzene is predominantly physisorbed at cryogenic temperature (100K) and chemisorbed at room temperature (300K).[20] Structure **2** was suggested as an adsorption product by the authors, even though they also observed the presence of another structure, proposed to be a tetra-σ bonded structure, on a timescale of hours.

As shown in this brief review of the previous works, several issues are still not clearly understood, especially, the configuration of the most stable product. The use of different experimental tools generated different results, and even similar STM techniques were

interpreted differently.[15-19] Various theoretical models were also applied to this system, yet the questions still seem to remain unresolved. Therefore, the current work presents a comprehensive *ab initio* study of the adsorption of benzene on Si(100). This includes the initial adsorption mechanisms, relative energetics of the products, and inter-conversion reactions among these products.

Computational Details

All calculations reported here were performed with the GAMESS (General Atomic and Molecular Electronic Structure System) electronic structure program.[22] A mixed basis set, consisting of the 6-31G(d) all electron basis[23] for carbon and hydrogen atoms and the HW(d) effective core potential (ECP) basis[24] for silicon atoms, was used. To assess the reliability of this mixed basis set, an all electron basis set, DZV(d) consisting of the Dunning-Hay double zeta valence basis plus d polarization functions, was also employed.[25] The Hessian matrix (matrix of energy second derivatives) was computed and diagonalized for all stationary points to characterize them. Intrinsic reaction coordinate (IRC) calculations, using the Gonzalez-Schlegel second-order method,[26] were conducted to verify that the saddle point connects the two minima of interest.

In order to describe benzene on Si(100) properly, the use of adequate wave functions is critical, because most of the adsorption products have at least one diradicaloid bare Si-Si dimer or conjugated (or just simple) π bond in which the gap between the bonding and the anti-bonding orbitals is close enough to allow configurational mixing. It is now well-established that the Si(100) bare surface can only be correctly described with multi-reference wave functions, since this was first pointed out by Redondo and Goddard.[27-32] In addition, benzene loses its aromaticity during the adsorption process, and some of the delocalized π orbitals are converted to Si-C σ orbitals. Redistribution of this aromatic stabilization energy into newly formed σ bonds can only be correctly described by multi-reference wave functions. Therefore, since there are 4 active electrons and 4 dangling bonds in two silicon dimers and 6 active electrons and 6 delocalized π orbitals in the benzene molecule, CASSCF(10,10) wave functions (10 electrons in 10 orbitals complete active space SCF) are

consistently used throughout the paper. To recover dynamic electron correlation, single point energy calculations with the MCQDPT2 (multi-configurational quasi-degenerate second-order perturbation theory) method[33] were performed at the CASSCF(10,10) optimized geometries. This is denoted by MCQDPT2//CASSCF(10,10).

A two dimer $Si_{31}H_{28}$ cluster was used to model the Si(100) surface because the benzene molecule is large enough to bridge across two dimers. However, $Si_{31}H_{28}/C_6H_6$ is a rather large system for multi-reference perturbation theory methods. As an alternative, hybrid QM/MM (quantum mechanics/ molecular mechanics) methods are becoming popular for modeling large molecular systems. In the QM/MM method, the chemically inactive region of the system is replaced by computationally inexpensive force field calculations, while the chemically active part, in which a reaction will occur, is still treated with full quantum mechanics. It has been shown that the SIMOMM (surface integrated molecular orbital molecular mechanics)[34] QM/MM method gives reasonable results with relatively low computational cost.[29,31,32] In this work, the benzene molecule and the top two layers of the surface (10 silicon atoms in uppermost layers and corresponding terminating hydrogen atoms) are described by quantum mechanics, and the rest of the surface (21 bulk silicon atoms and corresponding terminating hydrogen atoms) by molecular mechanics (In Chart 1, the QM atoms are in green and the MM atoms in gray).

Results and Discussion

A. Adsorption products and their relative energetics

Five potential candidates (**1**-**5**) suggested in the previous DFT//HF study as reaction products were examined.[15-17] Table 1 summarizes the relative energies of the products. At the CASSCF(10,10) level of theory, only structures **2** and **3** are found to be bound (negative binding energy) relative to the reactant. However, with the MCQDPT2 single point energy corrections at the same geometries, **1**, **2**, **3**, and **4** are determined to be bound, while **5** is still unbound with respect to the reactant. This is consistent with the previous DFT//HF results.[17] Regardless of the adsorption products, there are two opposing forces affecting the stabilities (binding energies) of the products: the breaking of aromatic stability of benzene during

adsorption, and some newly forming σ bonds between Si and C. Considering that all products except for **5** have negative binding energies at the MCQDPT2//CASSCF(10,10) level of theory, the formation of new Si-C σ bonds appear to be more important than the loss of aromaticity as a driving force for the reaction. However, the creation of two radical centers in **5** upon adsorption makes this structure unstable relative to the reactant, even though **5** has four Si-C σ bonds. Accordingly, **5** is not considered in the remainder of this paper.

Both CASSCF(10,10) and MCQDPT2//CASSCF(10,10) results consistently predict **2** to be the global minimum, although the preference for **2** relative to **3** is small when dynamic correlation is included. The di-σ bonded structures, **1** and **2**, are similar to the [2+2] and [4+2] (i.e., Diels-Alder) cycloaddition products, respectively, even though both surface reactions involve the breaking of the aromaticity of benzene. It is well known that the [4+2] products are more stable than the [2+2] products. This is not only because the [2+2] cycloaddition is a symmetry forbidden reaction (kinetics), but also because the six-membered ring produced by the [4+2] cycloaddition has less ring strain than the four-membered ring produced by the [2+2] cycloaddition (thermodynamics). Thus, it seems to be natural that **2** is more stable than **1**.

Isomers **3** and **4** are the tetra-σ bonded structures. By forming two more σ bonds than **1** and **2**, they can potentially gain extra stabilization. However, in order to form those additional bonds, the surface cannot avoid some degree of distortion. The dimer-dimer distances are 3.93, 3.94, and 3.95 Å for the bare cluster, **1** and **2**, respectively. However, **3** and **4** have inter-dimer distances of 3.33 and 3.35Å (and 3.68Å), respectively, distorting the surface substantially. Thus, this twisting of the surface (increasing the energy) and the formation of additional σ bonds (decreasing the energy) are opposing forces in **3** and **4**. Since **3** has a comparable binding energy to **2**, it is likely that these two factors cancel each other in **3**. On the other hand, the surface structure in **4** is more distorted than that in **3**, and thus **4** is much less stable than **3**.

In order to assess the reliability of the 'mixed' basis set consisting of 6-31G(d) for carbon and hydrogen, and HW(d) for silicon, all electron calculations with the DZV(d) basis were performed. As shown in Table 1, the two basis sets give very similar results, predicting

2 to be the global minimum and **3** very close to **2** in stability. These results, however, disagree with previous single-reference calculations (restricted Hartree-Fock or density functional theory) or semi-empirical predictions, in which **3** was predicted to be the lowest energy structure (Table 1). This implies that mult-reference character of the reactant, and **1** and **2** requires a multi-reference description.

The CASSCF(10,10) natural orbital occupations numbers for the structures in Chart 1 are listed in Table 2. Large occupation numbers for the active antibonding orbitals of **1** and **2** suggest that multi-reference character of **1** and **2**, as well as that of the reactants, is more significant than that of **3** and **4**. Consequently, the single reference methods will tend to over-emphasize the relative stabilities of **3** and **4**. Therefore, we conclude that the multi-reference wave functions must be used to correctly and consistently describe the potential energy surface of benzene on the Si(100) surface. However, considering the fact that **2** and **3** differ by only a few kcal/mol, the relative energies of these two species could change if one examined the potential energy surface with MCQDPT2 geometries and increased the size of the basis set.

B. Initial adsorption mechanisms

In this section, the adsorption mechanisms for the di-σ bonded structures, **1** and **2,** are discussed. Inter-conversion reactions among all products, including the formation of **3** and **4**, are in progress.

[4+2] Cycyoaddition mechanism. Structure **2** is a symmetry-allowed [4+2]-like cycloaddition adduct, and thus one expects a small or zero reaction barrier for the formation of **2** from the reactants. However, the CASSCF(10,10) barrier is calculated to be 17.7 kcal/mol. The stationary point **8** (See Chart1) at this barrier is a true transition state, as characterized by the CASSCF(10,10) Hessian matrix. However, subsequent MCQDPT2 single point energy calculations on the reactant, **8**, and **2** result in the prediction that **8** has a lower energy than the reactant. This could either mean that there is really no barrier (and that structure **8** is not a stationary point) at the higher level of theory, or that the MCQDPT2 transition state geometry is very different from that predicted by CASSCF(10,10). In order to shed some light on this, a series of MCQDPT2 single point calculations were performed

along the CASSCF(10,10) IRC. The results are presented in Figure 1. The MCQDPT2 energies decrease almost monotonically as the geometry changes along the CASSCF(10,10) minimum energy path from the reactant to **2**. Therefore, while the complete MCQDPT2 potential energy surface is not currently obtainable, the MCQDPT2//CASSCF(10,10) level of theory calculations suggest that the [4+2] addition of benzene on the Si(100) surface occurs with little or no barrier. This result is in accordance with the usual [4+2] cycloaddition energetics (a small or zero reaction barrier).

The fact that a 17.7 kcal/mol CASSCF(10,10) reaction barrier essentially disappears at the MCQDPT2//CASSCF(10,10) level of theory further suggests that dynamic electron correlation is very important for this system. However, since the analytic gradient codes for the MCQDPT2 method is not currently available, only the single point energy corrections are recovered in the present work. Nonetheless, it is clear that for a correct description of the entire potential energy surface of this system, both dynamic and non-dynamic electron correlation must be considered.

[2+2] Cycloaddition mechanism. The [2+2] cycloaddition is symmetry-forbidden according to the Woodward-Hoffmann rules. However, it has been shown that the [2+2] reaction for 1,3-cyclohexadiene on the Si(100) surface can also occur if the reaction follows a nonsymmetric pathway.[13] At the CASSCF(10,10) level of theory, an asymmetric transition state, **7**, was located for the [2+2] cycloaddition of benzene on Si(100). No symmetric reaction path was found. The reaction barrier is determined to be 16.0 kcal/mol at the MCQDPT2//CASSCF(10,10), and 23.6 kcal/mol at the CASSCF(10,10) level of theory. Compared to the [2+2] cycloaddition of 1,3-cyclohexadiene on the Si(100) surface (~8 kcal/mol at the MCQDPT2//CASSCF(6,6)/HW(d)),[31] this barrier is somewhat larger. This discrepancy may be due to the fact that the [2+2] addition of our system entails the breaking of the aromaticity of benzene, thereby making it more difficult for the reaction to occur.

The CASSCF(10,10) occupation numbers of the active orbitals at the [2+2] transition state, **7**, (Table 2) exhibit more significant multi-reference character than any other stationary point. Occupation numbers 1.47 (0.53) and 1.69 (0.31) correspond to bonding (anti-bonding) orbitals for the newly forming C_1-Si_1 bond and the bare silicon dimer, respectively. Again,

such large anti-bonding orbital occupation numbers suggest that a single reference method cannot describe this system correctly. The bond length, 2.35 Å, for the reacting silicon dimer (**7** in Chart 1) indicates that this moiety loses its diradical character at the transition state. The clean surface dimer has a bond length of 2.24-2.28 Å depending on the cluster size used at the CASSCF level of theory, and 2.24 Å according to experiment.[29,35]

Conclusions

A comprehensive *ab initio* study of the adsorption of benzene on the Si(100) surface has been presented. The [4+2] structure is predicted to be the lowest energy product. This result is inconsistent with previous single reference results (restricted Hartree-Fock or density function theory) in which **3** was suggested to be the lowest energy structure. This suggests that a mult-reference wave function is necessary for a proper description of this potential energy surface. The CASSCF(10,10) natural orbital occupation numbers for the active orbitals used in the calculations confirm the need for multi-reference wave functions.

At the highest level of theory, it is predicted that there is no reaction barrier for the [4+2] cycloaddition of benzene on the Si(100) surface, even though the reaction involves the loss of benzene aromaticity. Comparison of the MCQDPT2 single points potential energy surface and the CASSCF(10,10) potential energy surface for the [4+2] cycloaddition mechanism illustrates that dynamic electron correlation is very important for this system. The [2+2] addition of benzene on Si(100) can also occur via an asymmetric pathway with a reaction barrier of 16 kcal/mol.

The degree of surface distortion and the number of newly formed Si-C σ-bonds are the two main factors determining the stabilities (binding energies) of the products. Isomers **2** and **3** are predicted to have very similar binding energies, whereas **4** is less stable than **3** because **4** has a more twisted surface structure. Isomer **5** is predicted to be unbound relative to the reactant because it has two radical centers.

The comparison of the mixed basis results with the all electron DZV(d) basis results demonstrated that the mixed basis gives essentially the same results as the all electron basis with a relatively low computational effort.

Acknowledgment

This work was supported by a grant from the Air Force Office of Scientific Research. The calculations were performed on an Alpha Cluster, obtained by grants from the Department of Energy and the National Science Foundation. The authors thank Dr. Cheol Ho Choi for many helpful discussions.

References

1. G. P. Lopinski, D. J. Moffatt, D. D. M. Wayner, R. A. Wolkow, Am. Chem. Soc. **122**, 3548 (2000)
2. J. Yoshinobu, H. Tsuda, M. Onchi, and M. Nishijima, J. Chem. Phys. **87**, 7332 (1987)
3. W. Widdra, C. Huang, and W. H. Weinberg, Surf. Sci. **329**, 295 (1995)
4. W. Widdra, C. Huang, S. I. Yi, and W. H. Weinberg, J. Chem. Phys. **105**, 5605 (1996)
5. M. Nishijima, J. Yoshinobu, H. Tsuda, and M. Onchi, Surf. Sci. **192**, 383 (1987)
6. Y. Imamura, Y. Morikawa, T. Yamasaki, and H. Nakatsuji, Surf. Sci. **341**, L1091 (1995)
7. Q. Liu and R. Hoffmann, J. Am. Chem. Soc. **117**, 4082 (1995)
8. L. Li, C. Tindall, O. Takaoka, Y. Hasegawa, and T. Sakurai, Phys. Rev. B **56**, 4648 (1997)
9. R. A. Wolkow, Annu. Rev. Phys. Chem. **50**, 413 (1999)
10. Y. Taguchi, M. Fujisawa, T. Takaoka, T. Okada, and M. Nishijima, J. Chem. Phys. **95**, 6870 (1991)
11. B.I. Craig, Surf. Sci. **280**, L279 (1993)
12. H. D. Jeong, S. Ryu, Y. S. Lee, and S. Kim, Surf. Sci. **344**, L1226 (1995)
13. U. Birkenheuer, U. Gutdeutch, and N. Rosch, Surf. Sci., **409**, 213 (1998)
14. S. Gokhale, P. Trischberger, D. Menzel, W. Widdra, H. Droge, H.-P. Steinruck, U. Birkenheuer, U. Gutdeutsch, and N. Rosch, J. Chem. Phys. **108**, 5554 (1998)
15. G.P. Lopinski, D. J. Moffatt, and R. A. Wolkow, Chem. Phys. Lett. 282, 305 (1998)
16. G. P. Lopinski, T. M. Fortier, D. J. Moffat, and R. A. Wolkow, J. Vac. Sci. Technol. A **16** 1037 (1998)
17. R. A. Wolkow, G.P. Lopinski, and D. J. Moffatt, Surf. Sci. Lett. **416**, L1107 (1998)
18. B. Borovsky, M. Krueger, and E. Ganz, Phys. Rev. B **57**, R4269 (1998)
19. K. W. Self, R. I. Pelzel, J. H. G. Owen, C. Yan, W. Widdra, and W. H. Weinberg, J. Vac. Sci. Technol. A **16**, 1031 (1998)
20. M. J. Kong, A. V. Teplyakov, J. F. Lyubovitsky, and S. F. Bent, Surf. Sci. **411**, 286 (1998)
21. P. L. Silvestrelli, F. Ancilotto, and F. Toigo, Phys. Rev. B **62**, 1596 (2000)

22. M. W. Schmidt, K. K. Baldridge, J. A. Boatz, S. T. Elbert, M. S. Gordon, J. H. Jensen, S. Koseki, N. Matsunaga, K. A. Nguyen, S. Su, T. L. Windus, M. Dupuis, and J. A. Montgomery, Jr., J. Comput. Chem. **14**, 1347 (1993)
23. W. J. Hehre, R. Ditchfield, and J. A. Pople, J. Chem. Phys. **56**, 2257 (1972); M. M. Francl, W. J. Pietro, W. J. Hehre, J. S. Binkley, M. S. Gordon, D. J. Defrees, and J. A. Pople, *ibid.* **77**, 3654 (1982)
24. P. J. Hay and W. R. Wadt, J. Chem. Phys. **82**, 270 (1985)
25. T. H. Dunning and P. J. Hay, In *Methods of Electronic Structure Theory*, H. F. Schaefer III, Ed., Plenum Press, New York (1977)
26. C. Gonzalez, H. B. Schegel, J. Chem. Phys. **95**, 5853 (1991)
27. A. Redondo, and W. A. Goddard III, J. Vac. Sci. Technol. **21**, 344 (1982)
28. B. Paulus, Surf. Sci. **375**, 55 (1997)
29. J. Shoemaker, J. W. Burggraf, and M. S. Gordon, J. Chem. Phys. **112**, 2994 (2000)
30. M. S. Gordon, J. R. Shoemaker, and L. W. Burggraf, J. Chem. Phys. **113**, 9355 (2000)
31. C. H. Choi, and M. S. Gordon, J. Am. Chem. Soc. **121**, 11311 (1999)
32. Y. Jung, C. H. Choi, and M. S. Gordon, J. Phys. Chem. B **105**, 4039 (2001)
33. H. Nakano, J. Chem. Phys. **99**, 7983 (1993)
34. J. Shoemaker, J. W. Burggraf, and M. S. Gordon, J. Phys. Chem. A **103**, 3245 (1999)
35. Y. Wang, M. Shi, and J. W. Rabalais, Phys. Rev. B **48**, 1689 (1993)

Table 1. Relative binding energies (kcal/mol) of the adsorption products for benzene on the Si(100) surface.

	Reactants	**1**	**2**	**3**	**4**	**5**
This work: SIMOMM ($Si_{31}H_{28}/C_6H_6$)						
CASSCF(10,10)/MIXED [a]	0	0.4	-16.7	-10.4	0.1	42.7
MCQDPT2//CASSCF(10,10)/MIXED [a]	0	-3.9	-25.5	-24.4	-12.0	27.3
CASSCF(10,10)/DZV(d)	0	0.3	-17.3	-8.5	-1.6	
MCQDPT2//CASSCF(10,10)/DZV(d)	0	-6.3	-29.0	-26.7	-14.5	
Previous works						
Car-Parrinello MD/BLYP [b]	0	-17.8	-28.1	-35.3	-30.2	
DFT/B3LYP/6-31G(d)//HF/3-21G(d) [c]	0	-3.9	-20.2	-34.4	-21.0	

[a] Mixed basis set: HW(d) for Si and 6-31G(d) for H and C.

[b] Using a periodic slab model, reference 21

[c] Using a $Si_{15}H_{16}$ cluster model, reference 17

Table 2. CASSCF(10,10) natural orbital occupation numbers (NOON) for the structures in Chart 1, corresponding to the five active bonding orbitals (values in parentheses are occupation numbers for the corresponding anti-bonding orbtials).

Structures	NOON				
Reactants	1.68 (0.32)	1.70 (0.30)	1.90 (0.10)	1.90 (0.10)	1.95 (0.05)
1	1.69 (0.31)	1.88 (0.12)	1.93 (0.07)	1.97 (0.03)	1.98 (0.02)
2	1.69 (0.31)	1.91 (0.09)	1.92 (0.08)	1.98 (0.02)	1.98 (0.02)
3	1.92 (0.08)	1.97 (0.03)	1.97 (0.03)	1.98 (0.02)	1.98 (0.02)
4	1.92 (0.08)	1.97 (0.03)	1.97 (0.03)	1.97 (0.03)	1.97 (0.03)
5	1.31 (0.69)	1.97 (0.03)	1.97 (0.03)	1.97 (0.03)	1.97 (0.03)
7	1.47 (0.53)	1.69 (0.31)	1.89 (0.11)	1.93 (0.07)	1.98 (0.02)
8	1.69 (0.31)	1.82 (0.18)	1.90 (0.10)	1.91 (0.09)	1.96 (0.04)

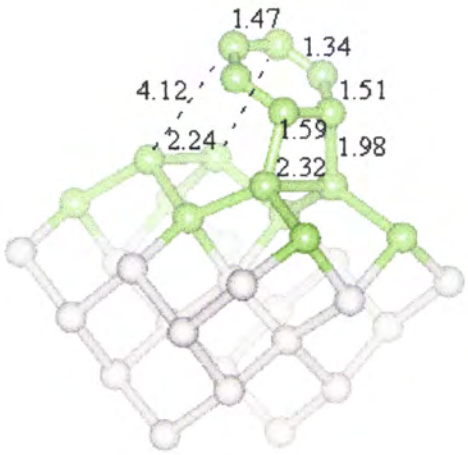

1

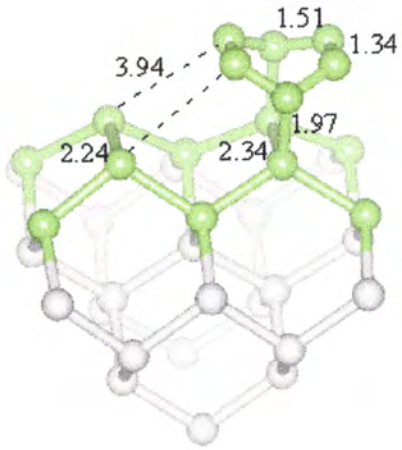

2

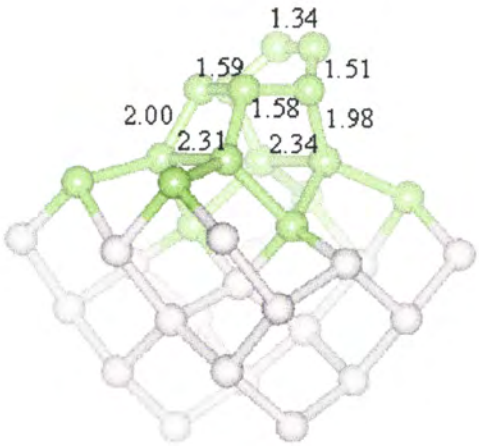

3

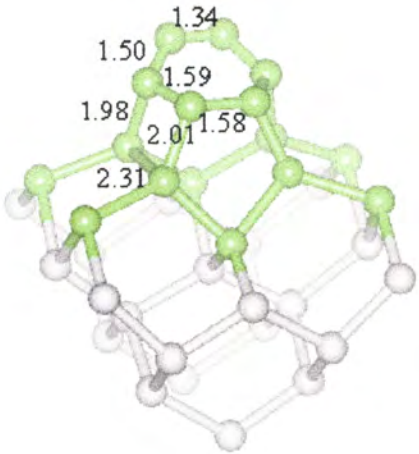

4

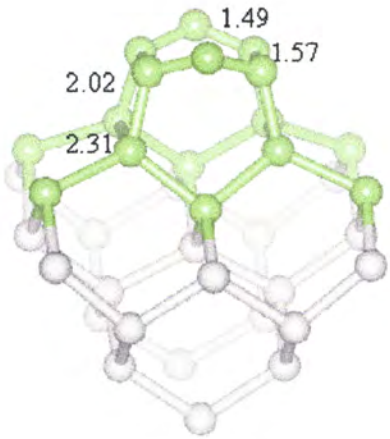

5

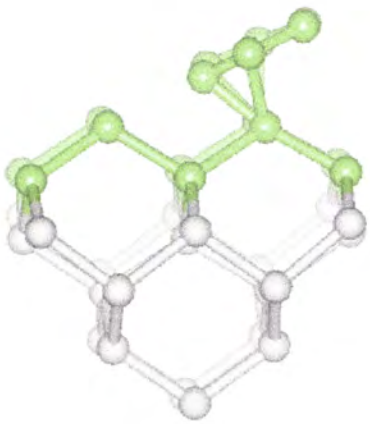

6

Chart 1

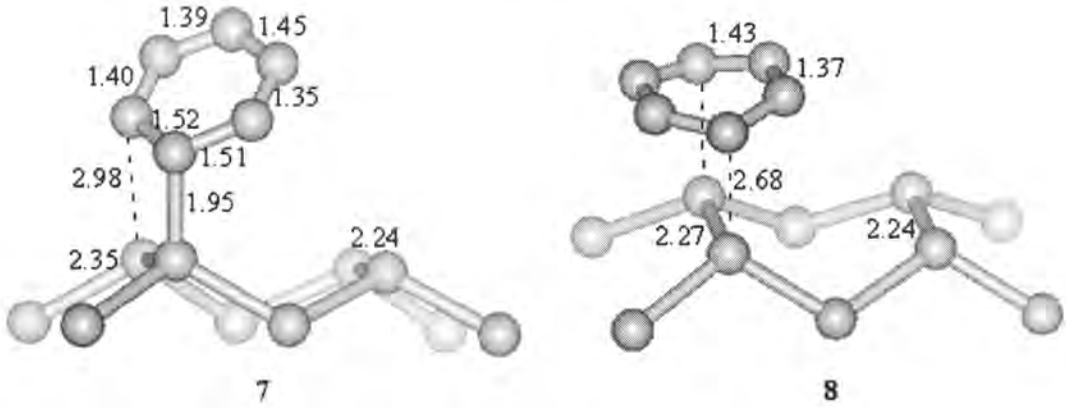

7 8

Chart 1 (continued)

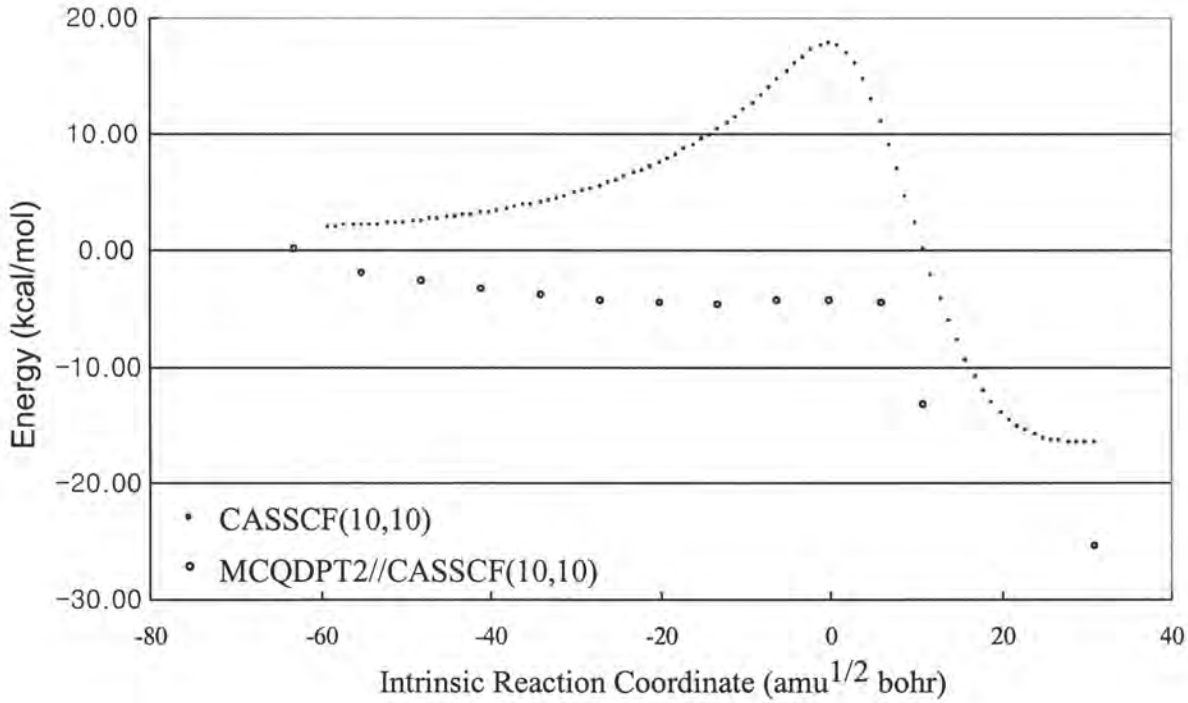

Figure 1. Potential energy curve for the [4+2] cycloaddition mechanism

CHAPTER 5. THE MODIFICATION OF THE HESSIAN MODULE OF THE SIMOMM METHOD

Introduction

The need for modeling large molecular systems such as biological species or surfaces is becoming increasingly important. The use of quantum mechanics for such complex systems has been limited because of the computational intractability in calculating them. Linear scaling techniques attempt to apply quantum mechanics to such large molecular systems by scaling the computational effort linearly with molecular size, because high-order scaling has been a barrier to the application of traditional quantum mechanics to large systems.[1-3] An alternative way of modeling large systems is to use hybrid QM/MM (quantum mechanics/molecular mechanics) techniques.

In QM/MM methods,[4-7] the total system is divided into two parts: a chemically active region in which a reaction will occur, and a chemically inactive region that frequently represents the solvent or the bulk. The chemically active part is modeled with quantum mechanics and the chemically inactive part with molecular mechanics. The purpose of the MM part is to provide a model potential that represents the potential of the bulk in a simple form, and to give geometrical constraint to the active region. Maseras and Morokuma developed a hybrid QM/MM method called IMOMM (integrated molecular orbital molecular mechanics).[7] In IMOMM, the energy gradients (the forces) from QM and MM parts are combined to generate hybrid gradients, and these hybrid gradients are used to find the next point in a geometry optimization. However, the fixed user selected geometric parameters for the link atoms in IMOMM can lead to inaccurate geometry predictions. This is especially the case when it is used in surface modeling, because the high degree of connectivity in a lattice will introduce a large number of user defined constraints.

The SIMOMM (surface integrated molecular orbital molecular mechanics) is a modification[8] of the IMOMM scheme, in which all the geometry constraints imposed in IMOMM are removed. It has been shown that the SIMOMM method gives reasonable results with relatively low computational cost.[12-15]

The calculation of the energy second derivatives with respect to the nuclear coordinates (the Hessian matrix) is crucial to characterize the optimized geometry on a potential energy surface to determine, for example, whether the structure is a transition state or a minimum. Currently, a SIMOMM Hessian is determined numerically as follows:

$$\underline{\underline{H}} = \begin{pmatrix} H_{11} & H_{12} & \cdots & H_{1,3N} \\ H_{21} & \ddots & & \vdots \\ \vdots & & \ddots & \vdots \\ H_{3N,1} & \cdots & \cdots & H_{3N,3N} \end{pmatrix} = \begin{pmatrix} \frac{\partial^2 E}{\partial x_1^{\,2}} & \frac{\partial^2 E}{\partial x_1 \partial y_1} & \frac{\partial^2 E}{\partial x_1 \partial z_1} & \cdots & \frac{\partial^2 E}{\partial x_1 \partial z_N} \\ \frac{\partial^2 E}{\partial y_1 \partial x_1} & & & & \\ \frac{\partial^2 E}{\partial z_1 \partial x_1} & & \ddots & & \vdots \\ \vdots & & & & \\ \frac{\partial^2 E}{\partial z_N \partial x_1} & & \cdots & & \frac{\partial^2 E}{\partial x_N \partial z_N} \end{pmatrix}$$

$$= \begin{pmatrix} \frac{\partial}{\partial x_1}\left(\frac{\partial E}{\partial x_1}\right) & \frac{\partial}{\partial y_1}\left(\frac{\partial E}{\partial x_1}\right) & \frac{\partial}{\partial z_1}\left(\frac{\partial E}{\partial x_1}\right) & \cdots & \frac{\partial}{\partial z_N}\left(\frac{\partial E}{\partial x_1}\right) \\ \frac{\partial}{\partial x_1}\left(\frac{\partial E}{\partial y_1}\right) & \frac{\partial}{\partial y_1}\left(\frac{\partial E}{\partial y_1}\right) & & & \\ \frac{\partial}{\partial x_1}\left(\frac{\partial E}{\partial z_1}\right) & & \ddots & & \vdots \\ \vdots & & & & \\ \frac{\partial}{\partial x_1}\left(\frac{\partial E}{\partial z_N}\right) & & \cdots & & \frac{\partial}{\partial z_N}\left(\frac{\partial E}{\partial z_N}\right) \end{pmatrix}$$

$$= \begin{pmatrix} \frac{\partial}{\partial x_1}\vec{g} & \frac{\partial}{\partial y_1}\vec{g} & \frac{\partial}{\partial z_1}\vec{g} & \cdots & \frac{\partial}{\partial z_N}\vec{g} \end{pmatrix}$$

$$= \begin{pmatrix} \frac{\vec{g}_{11} - \vec{g}_0}{\delta x_1} & \frac{\vec{g}_{12} - \vec{g}_0}{\delta y_1} & \frac{\vec{g}_{13} - \vec{g}_0}{\delta z_1} & \cdots & \frac{\vec{g}_{N3} - \vec{g}_0}{\delta z_N} \end{pmatrix}$$

where, the equilibrium coordinates are $\left(x_1^{eq}, y_1^{eq}, z_1^{eq}, x_2^{eq}, y_2^{eq}, z_2^{eq}, \cdots, x_N^{eq}, y_N^{eq}, z_N^{eq}\right)$

$$\vec{g}^{\,T} = \left(\frac{\partial E}{\partial x_1} \quad \frac{\partial E}{\partial y_1} \quad \frac{\partial E}{\partial z_1} \quad \cdots \quad \frac{\partial E}{\partial z_N} \right)$$

$$\vec{g}_0{}^{T} = \left(\frac{\partial E}{\partial x_1}, \frac{\partial E}{\partial y_1}, \frac{\partial E}{\partial z_1}, \frac{\partial E}{\partial x_2}, \cdots, \frac{\partial E}{\partial z_N} \right)_{x_1^{eq}, y_1^{eq}, z_1^{eq}, x_2^{eq}, y_2^{eq}, z_2^{eq}, \cdots, x_N^{eq}, y_N^{eq}, z_N^{eq}}$$

$$\vec{g}_{11}{}^{T} = \left(\frac{\partial E}{\partial x_1}, \frac{\partial E}{\partial y_1}, \frac{\partial E}{\partial z_1}, \frac{\partial E}{\partial x_2}, \cdots, \frac{\partial E}{\partial z_N} \right)_{x_1^{eq} + \delta x_1, y_1^{eq}, z_1^{eq}, x_2^{eq}, y_2^{eq}, z_2^{eq}, \cdots, x_N^{eq}, y_N^{eq}, z_N^{eq}}$$

$$\vec{g}_{12}{}^{T} = \left(\frac{\partial E}{\partial x_1}, \frac{\partial E}{\partial y_1}, \frac{\partial E}{\partial z_1}, \frac{\partial E}{\partial x_2}, \cdots, \frac{\partial E}{\partial z_N} \right)_{x_1^{eq}, y_1^{eq} + \delta y_1, z_1^{eq}, x_2^{eq}, y_2^{eq}, z_2^{eq}, \cdots, x_N^{eq}, y_N^{eq}, z_N^{eq}}$$

$$\vec{g}_{13}{}^{T} = \left(\frac{\partial E}{\partial x_1}, \frac{\partial E}{\partial y_1}, \frac{\partial E}{\partial z_1}, \frac{\partial E}{\partial x_2}, \cdots, \frac{\partial E}{\partial z_N} \right)_{x_1^{eq}, y_1^{eq}, z_1^{eq} + \delta z_1, x_2^{eq}, y_2^{eq}, z_2^{eq}, \cdots, x_N^{eq}, y_N^{eq}, z_N^{eq}}$$

, and so on.

In actual calculations, the infinitesimal displacements are taken as $\delta x_1 = \delta y_1 = \delta z_1 = \delta x_2 = \cdots = \delta$, and 0.01 Bohr was used in this study. $\vec{g}_0$ is the gradient vector at equilibrium geometry, and $\vec{g}_{AB}$ represents the gradient vector at infinitesimally displaced geometry (i.e., B^{th} component – x, y, or z - of atom A is displaced by δ). This numerical algorithm utilizing gradients (the first derivatives) to calculate the second derivatives matrix is called the finite differencing method. Lastly, since the force constant matrix should be symmetric, for example, $\frac{\partial}{\partial y_1}\left(\frac{\partial E}{\partial x_1}\right) = \frac{\partial}{\partial x_1}\left(\frac{\partial E}{\partial y_1}\right)$, those matrix elements that are supposed to have the same value are averaged. In order words, $H_{12}{}' = H_{21}{}' = \frac{1}{2}(H_{12} + H_{21})$, $H_{13}{}' = H_{31}{}' = \frac{1}{2}(H_{13} + H_{31})$, etc. Finally, the symmetric Hessian

matrix is diagonalized, and the vibrational frequencies are calculated from the eigenvalues of the Hessian matrix.

In the current version of SIMOMM implemented in GAMESS (general atomic and molecular electronic structure system),[9] however, only the QM part is considered in the foregoing numerical steps. In other words, only QM atoms are displaced in the above procedure (*N* in the above equations is the number of QM atoms plus the terminating hydrogen atoms). However, the geometry optimization of SIMOMM utilizes not only the QM atoms but also the MM atoms through the gradients of MM atoms. Thus, the calculation of the energy second derivatives should also include the effect of the MM atoms in its numerical steps to be more consistent with the geometry optimization scheme.

Therefore, in this study, the influence of including MM displacements in the original SIMOMM method of numerical Hessian routine is considered, and the results are presented.

Computational models

The Si_9H_{12} surface clusters modified with the second row organic functional groups (e.g., CH_3, NH_2, OH, F) are used for the test of the new method. The restricted Hartree-Fock method with 6-31G(d) basis,[10] denoted by RHF/6-31G(d), was used. 0.89 was used for the scaling factor of the frequency results.[11] The results with the new method were compared with those obtained from the full quantum mechanical calculation and those from the original SIMOMM method.

Results and discussion

The second row elements (-CH_3, -NH_2, -OH, and -F) were used to terminate the other end of the surface dimer while capping one end with hydrogen. Vibrational frequencies (eigenvalues of the Hessian matrix) were calculated, and the results are summarized in Tables 1-4. The geometries were first optimized using the original SIMOMM method to locate the global minimum. These structures were then used for the frequency calculations using both the original and new SIMOMM methods. Only a subset of interesting vibrations in the QM region were considered and compared.

In general, no large differences between the original and new methods are observed. The largest difference is 20 cm^{-1}, and the differences in most of the vibrations are less than 10 cm^{-1}. The results also show that the original SIMOMM method yields slightly closer results to the full QM results than the new method, even though both methods give essentially the same results. Thus, we conclude that the inclusion of MM atom displacements in the numerical Hessian calculation does not improve the results and gives similar results to the original method.

Conclusion

The numerical Hessian subroutine of the SIMOMM method was modified to include the effect of the MM atoms on the Hessian. The modified codes were tested using the vibrational frequency calculations for the second row elements ($-CH_3$, $-NH_2$, -OH, and -F) bonded to the Si_9H_{12} surface cluster model. The full QM results, original SIMOMM results, and the results from the new method were compared. The results for all cases consistently showed that the new SIMOMM Hessian method does not give any improvements over the original method in terms of the vibrational frequencies relative to the full QM results. However, including the motions of all atoms is more rigorously satisfying, and occasions may arise for which the new method is more accurate.

References

1. M. Challacombe and E. Schwegler, J. Chem. Phys. **106**, 5526 (1997)
2. C. A. White, B. G. Johnson, P. M. W. Gill, and M. Head-Gordon, Chem. Phys. Lett. **253**, 268 (1996)
3. C. H. Choi, J. Ivanic, M. S. Gordon, and K. Ruedenberg, J. Chem. Phys. **111**, 8825 (1999)
4. W. L. Jorgensen, J. Chandrasekhar, J. D. Madura, R. W. Impey, M. L. Klein, J. Chem. Phys. **79**, 926 (1983)
5. P. N. Day, J. H. Jensen, M. S. Gordon, S. P. Webb, W. J. Stevens, M. Krauss, D. Garmer, H. Basch, and D. Cohen, J. Chem. Phys. **105**, 1968 (1996)
6. B. Weiner, C. S. Carmer, and M. Frenklach, Phys. Rev. B **43**, 1678 (1991)
7. F. Maseras and K. Morokuma, J. Comput. Chem. **16**, 1170 (1995)
8. J. Shoemaker, L. W. Burggarf, and M. S. Gordon, J. Phys. Chem. A **103**, 3245 (1999)

9. M. W. Schmidt, K. K. Baldridge, J. A. Boatz, S. T. Elbert, M. S. Gordon, J. H. Jensen, S. Koseki, N. Matsunaga, K. A. Nguyen, S. Su, T. L. Windus, M. Dupuis, and J. A. Montgomery, Jr., J. Comput. Chem. **14**, 1347 (1993)
10. W. J. Hehre, R. Ditchfield, and J. A. Pople, J. Chem. Phys. **56**, 2257 (1972); M. M. Francl, W. J. Pietro, W. J. Hehre, J. S. Binkley, M. S. Gordon, D. J. Defrees, and J. A. Pople, *ibid.* **77**, 3654 (1982)
11. J. A. Pople, R. Krishnan, H. B. Schlegel, D. Defrees, J. S. Binkley, M. J. Frisch, R. F. Whiteside, R. F. Hout, and W. J. Hehre, Int. J. Quantum Chem., Symp. **15**, 269 (1981); J. A. Pople, A. P. Scott, M. W. Wong, and L. Radom, Israel J. Chem. **33**, 345 (1993)
12. C. H. Choi, and M. S. Gordon, J. Am. Chem. Soc. **121**, 11311 (1999)
13. Y. Jung, C. H. Choi, and M. S. Gordon, J. Phys. Chem. B **105**, 4039 (2001)
14. J. Shoemaker, J. W. Burggraf, and M. S. Gordon, J. Chem. Phys. **112**, 2994 (2000) M. S. Gordon, J. R. Shoemaker, and L. W. Burggraf, J. Chem. Phys. **113**, 9355 (2000)

Table 1. Some important vibrations for Si_9H_{13}-CH_3 (cm^{-1})

	Full QM	Original SIMOMM	New SIMOMM
Si-Si stretching	405	428	423
Si-H stretching	2059	2059	2059
Si-CH_3 stretching	1286	1288	1288
CH_3 asymmetric stretching 1	2914	2901	2900
CH_3 asymmetric stretching 2	2913	2919	2918
CH_3 symmetric stretching	2847	2838	2839

Table 2. Some important vibrations for Si_9H_{13}-NH_2 (cm^{-1})

	Full QM	Original SIMOMM	New SIMOMM
Si-Si stretching	420	436	437
Si-H stretching	2060	2059	2059
Si- NH_2 stretching	774	765	757
NH_2 asymmetric stretching	3444	3454	3454
NH_2 symmetric stretching	3360	3366	3366
H-N-H angle bending	1569	1573	1572

Table 3. Some important vibrations for Si_9H_{13}-OH (cm^{-1})

	Full QM	Original SIMOMM	New SIMOMM
Si-Si stretching	492	446	438
Si-H stretching	2076	2080	2081
Si-OH stretching	790	779	770
Si-O-H angle bending	834	831	827
O-H stretching	3669	3669	3668

Table 4. Some important vibrations for Si_9H_{13}-F (cm^{-1})

	Full QM	Original SIMOMM	New SIMOMM
Si-Si stretching	425	443	442
Si-H stretching	2072	2073	2073
Si-F stretching	812	809	829

CHAPTER 6. GENERAL CONCLUSION

Only a global summary will be presented in this chapter since the individual chapters include their own conclusions.

Two- and three-dimer clusters were used to investigate the structure of the Si(100) surface, and the results show that the surface dimers are symmetric within the frame of models and levels of theory used. However, it still remains as a question whether the models and the methods we used are sufficient to represent the actual surface. Therefore, future work on this subject should focus on the effect of using larger clusters on the structure of Si(100).

Reactions on the Si(100) surface, water and benzene, were studied. They are both barrierless or, at least, low-barrier reactions. Partial diradical (or double bond) character of the silicon (100) surface is the key to such surface phenomena. Thus, the use of adequate wave functions, from the theoretical point of view, is critical for the correct description of these surface reactions due to the multi-reference character of the surface dimers.

The SIMOMM method was effectively used for large cluster calculations throughout the thesis, and gave reasonable results with much less computational efforts compared to the full QM calculations. To be more consistent with the geometry optimization scheme in SIMOMM, numerical steps of the Hessian part of SIMOMM were slightly modified. Since the SIMOMM scheme has been shown to give reliable results in silicon chemistry, it would be desirable to adjust and apply the method to other metal systems also in future work.

ACKNOWLEDGMENTS

First and foremost, I would like to thank my family for their long distance support over the phone. Even though they sometimes woke me up in the middle of my deep sleep, not realizing the time difference between Ames and Korea, their encouragement was great.

I would especially like to thank my advisor, Dr. Mark Gordon, for his invaluable support and advice. Mark not only gave me academic advice; he also showed me a little bit of how to become a chemist. I would also like to thank all the Gordon group members for their helpful discussions and support. They all gave me a warm impression of America when I arrived in this endless cornfield two years ago!